

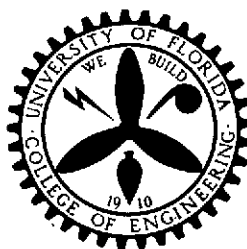
(NASA-CR-137359) MASS TRANSFER IN FUEL  
CELLS Semiannual report, 1 Mar - 31  
Aug. 1973 (Florida Univ.) 93 p HC \$7.75

N74-19696

CSC1 10B

Unclas

G3/03 16053



Reproduced by  
NATIONAL TECHNICAL  
INFORMATION SERVICE  
US Department of Commerce  
Springfield, VA. 22151



ENGINEERING AND INDUSTRIAL EXPERIMENT STATION

College of Engineering

University of Florida

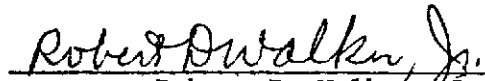
Gainesville

MASS TRANSFER IN FUEL CELLS

Research Grant NGL-10-005-022  
Sixteenth Semi-Annual Report  
Period Covered: March 1, 1973 - August 31, 1973

Prepared for  
National Aeronautics and Space Administration  
Washington, D.C.

December 14, 1973

  
Robert D. Walker, Jr.

ENGINEERING AND INDUSTRIAL EXPERIMENT STATION

College of Engineering  
University of Florida  
Gainesville, Florida

## TABLE OF CONTENTS

	<u>Page</u>
List of Tables .....	iv
List of Figures .....	v
 Sections:	
1. Summary .....	1
2. Surface Area and Pore Size Distribution .....	3
3. Electron Microscopy of Electrolyte Matrix Samples..	17
4. Distribution and Movement of Electrolyte in Fuel Cells .....	21
4.1 The Surface Tension of KOH Solutions.....	21
4.1.1 Experimental Methods.....	21
4.1.2 Preparation of Solutions.....	22
4.1.3 Experimental Results .....	23
4.1.4 The Data of Feldkamp .....	27
4.1.5 Discussion .....	36
4.2 Modelling of Wetting and Penetration of Porous, Heterogeneous Media .....	36
5. Water Transport In Alkaline $H_2-O_2$ Fuel Cells .....	37
5.1 Introduction .....	37
5.2 Mass Transfer in the Electrolyte Matrix.....	38
5.3 Transference Numbers in KOH Solutions .....	44
5.3.1 Methods for Measuring Transference Numbers .....	45
5.4 The Primary Hydration Number In Concentrated KOH Solutions .....	51
5.5 Concentration Gradients in the Electrolyte Matrix .....	57
5.6 Discussion of Simplifying Assumptions .....	61

TABLE OF CONTENTS (Continued)

	<u>Page</u>
6. Effectiveness Factors In Fuel Cell Components.....	62
6.1 Development of the Model .....	63
6.2 Proposed Equipment and Procedure .....	66
Appendices:	
1. Derivation of Flux Equations (Eq. 5.2-11 and 12)....	69
2. Derivation of Equation 5.2-16 .....	73
3. Sample Calculation of "Free" Water Concentration .....	77
4. Solution of the Diffusion Equation For the Effectiveness Factor Cell .....	79
List of References.....	86

# LIST OF TABLES

<u>Table</u>		<u>Page</u>
2.1	Surface Area and Pore Volume of Electrolyte Matrix Materials .....	13
2.2	Preferred Pore Sizes In Electrolyte Matrix Samples .....	13
2.3	Computer Analysis of Pore Size Distribution of Fuel Cell Electrolyte Matrix Materials .....	14
4.1	Surface Tension of KOH Solutions .....	25
4.2	a) Coefficients of the Correlations: $\sigma = B_1 + B_2 m + B_3 m^2$ .....	26
	b) Values Given By the Correlations .....	27
4.3	Matrix of Coefficients of the Feldkamp Equation .....	28
4.4	Coefficients of the Feldkamp Equation .....	30
4.5	Surface Tension of KOH Data From Feldkamp.....	31
5.1	Summary of Transference Number Data for KOH Solutions .....	51
5.2	Concentration of "Free" Water as a Function of Hydration Number .....	52
5.3	Primary Hydration Numbers of $K^+$ by Various Experimental Methods .....	54
5.4	Diffusivity of KOH Solution At 25°C .....	57
5.5	"Free" Water Concentration Gradients .....	58
5.6	KOH Concentration Gradients in the Electrolyte Matrix .....	60

# LIST OF FIGURES

<u>Figure</u>		<u>Page</u>
1	Pore Size Distribution of Asbestos-1 .....	4
2	Pore Size Distribution of Asbestos-2 .....	5
3	Pore Size Distribution of Asbestos-3 .....	6
4	Pore Size Distribution of Fybex-1 .....	7
5	Pore Size Distribution of Fybex-2 .....	8
6	Pore Size Distribution of Astropower Bag .....	9
7	Pore Size Distribution of 4D0573 Bag .....	10
8	Pore Size Distribution of 4D0573 Sheet.....	11
9	Pore Size Distribution of 11D2172 Sheet .....	12
10	Scanning Electron Micrographs of Uncoated Side of Electrolyte Matrices. 5000X .....	18
11	Scanning Electron Micrographs of Coated Side of Electrolyte Matrices. 2000X .....	19
12	Surface Tension of KOH Solutions .....	24
13	Surface Tension of KOH -- Concentration Dependence (Data From Feldkamp) .....	32
14	Surface Tension of KOH--Temperature Dependence (Data From Feldkamp) .....	33
15	Relative Surface Tension of KOH--Concentration Dependence (From Feldkamp) .....	34
16	Relative Surface Tension of KOH--Temperature Dependence (Data From Feldkamp) .....	35
17	Concentration of "Free" Water in KOH Solution For Different Degrees of Solvation .....	53

## 1. Summary

This report describes developments in the following areas: surface area and pore size distribution in electrolyte matrices, electron microscopy of electrolyte matrices, surface tension of KOH solutions, water transport in fuel cells, and effectiveness factors for fuel cell components.

The surface area and pore size distribution, as measured by nitrogen adsorption, have been determined for several electrolyte matrices made from asbestos or Fybex (fibrous potassium titanate), and for asbestos matrices impregnated with polyphenylene oxide with and without a coating of zirconia in polyphenylene oxide on one side. The specific surface areas found were: asbestos--44 m<sup>2</sup>/g; Fybex--16 m<sup>2</sup>/g; impregnated and coated asbestos--4 to 8 m<sup>2</sup>/g. Pore size distributions suggested that the Astropower bag (an impregnated and zirconia coated sample which appears to be somewhat superior for some purposes) had a more uniform distribution of pore sizes than any of the other samples. However, the most significant observation in this area is the large reduction in surface area which results from either impregnation or coating.

Scanning electron microscopy at a magnification of 2000 or 5000X suggested that the asbestos fiber bundles in the Astropower bag were more completely broken down than those in the other samples. It was also noted that the coating on the Astropower bag contained relatively large flat plates whereas the solid particles in the other coatings appeared to be much smaller and less platelike.

A recent paper which reported extensive surface tension data for KOH solutions was discovered just prior to preparation of this report. These new data correlate well both with our experimental data and those reported earlier. Data are correlated over a wide range of KOH concentrations and temperatures by a polynomial which utilizes a  $5 \times 5$  matrix of coefficients, but a computer is required for most calculations. A simpler correlation is being sought.

Traces of surface active impurities sharply reduce the surface tension of pure KOH solutions, and it is not clear at present whether surface tension data for pure KOH solutions are applicable for fuel cells.

The multicomponent diffusion equation has been solved for water transport in the electrolyte matrix for an  $H_2-O_2$  fuel cell with the assumptions of constant temperature and pressure (in the matrix) and no convection. Ionic hydration has been taken into account. While hydration results in significantly larger fluxes of water and hydroxyl ions for a given current density than is the case when hydration is ignored, the concentration gradients in the electrolyte matrix turn out to be quite small and even large errors in estimation of the primary hydration number of hydroxyl ion have relatively little influence on the concentration gradients.

A cell for measuring effectiveness factors of fuel cell components is under construction; it is based on a modification of the stagnant microelectrode. The differential equations for the cell have been solved and a computer program worked out to evaluate effective diffusivities from measurements of the limiting current.



## 2. Surface Area and Pore Size Distribution In Electrolyte Matrices--M. C. Lee

The surface area and pore size distribution were measured by the methods described in the Fifteenth Semi annual report for nine electrolyte matrix samples supplied by NASA. The samples studied bore the following designations: Fybex -1 and -2, Asbestos -1, -2 and -3, 4D0573 Sheet, and Bag, Astropower Bag, 11D2172 Sheet. The surface area and the apparent pore volume are shown in Table 2.1 and the pore size distribution curves in the pore size ranging up to about 20 nm in radius are given in Figures 1-9.

One can also measure the pore size distribution by other methods, notably by Mercury penetration. In this method, the volume of mercury intruded into the pores of a porous sample is measured at several pressures. From these data one can construct pore size distribution curves. It has been our experience that the mercury penetration technique appears to be suitable for the relatively rigid structures of electrodes, but that it leads to erroneous results for electrolyte matrices owing to their compressibility. It remains to be seen whether pore size distribution curves can be generated by mercury penetration measurements when the sample has been impregnated by PPO and then coated. This question will be explored in the near future.

The surface area and the apparent pore volume tests show significant differences between the three different kinds of sample groups. From the pore size distribution curves it can be seen that there are several preferred pore sizes and these are summarized in Table 2.2 below.

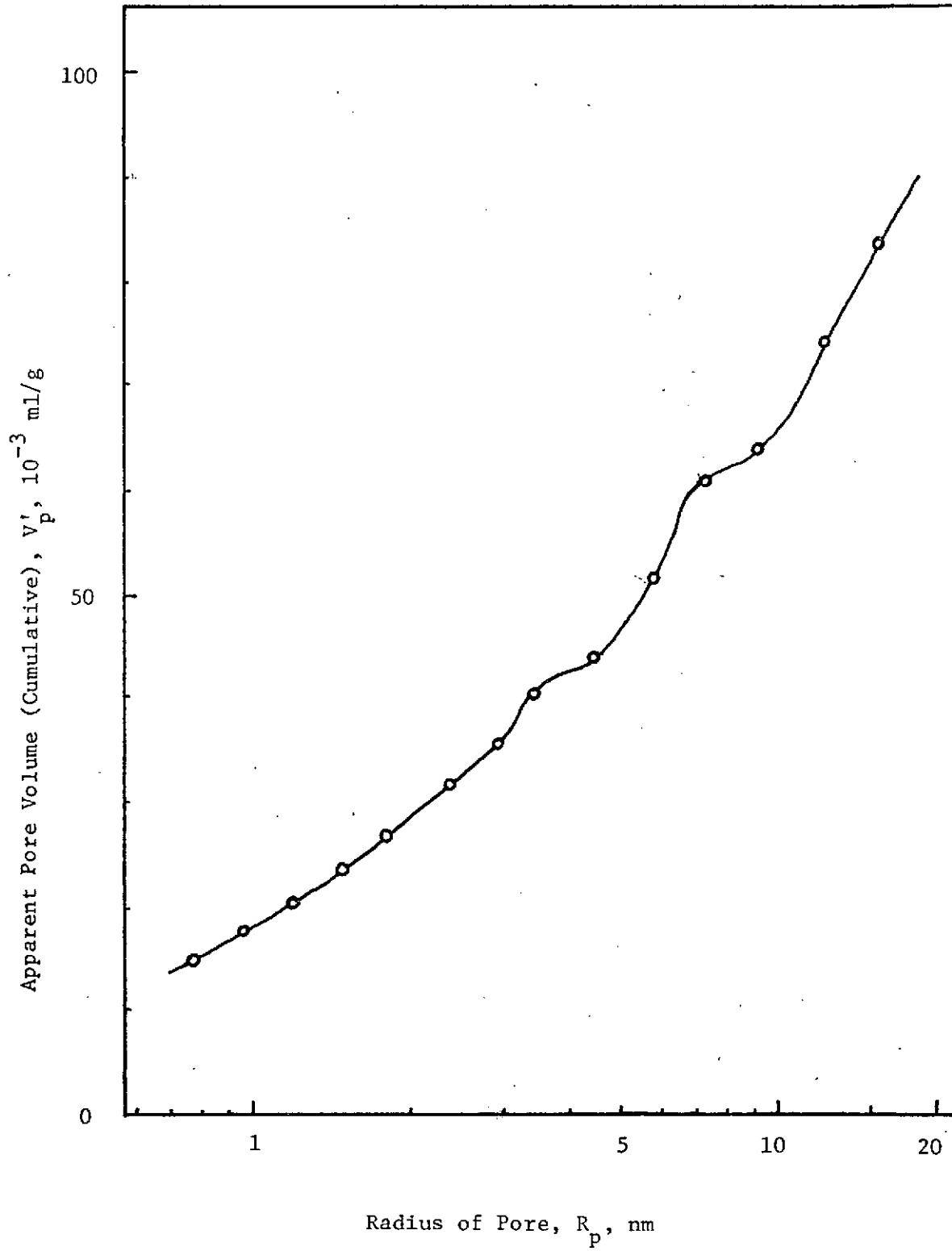


Figure 1: Pore Size Distribution of Asbestos-1

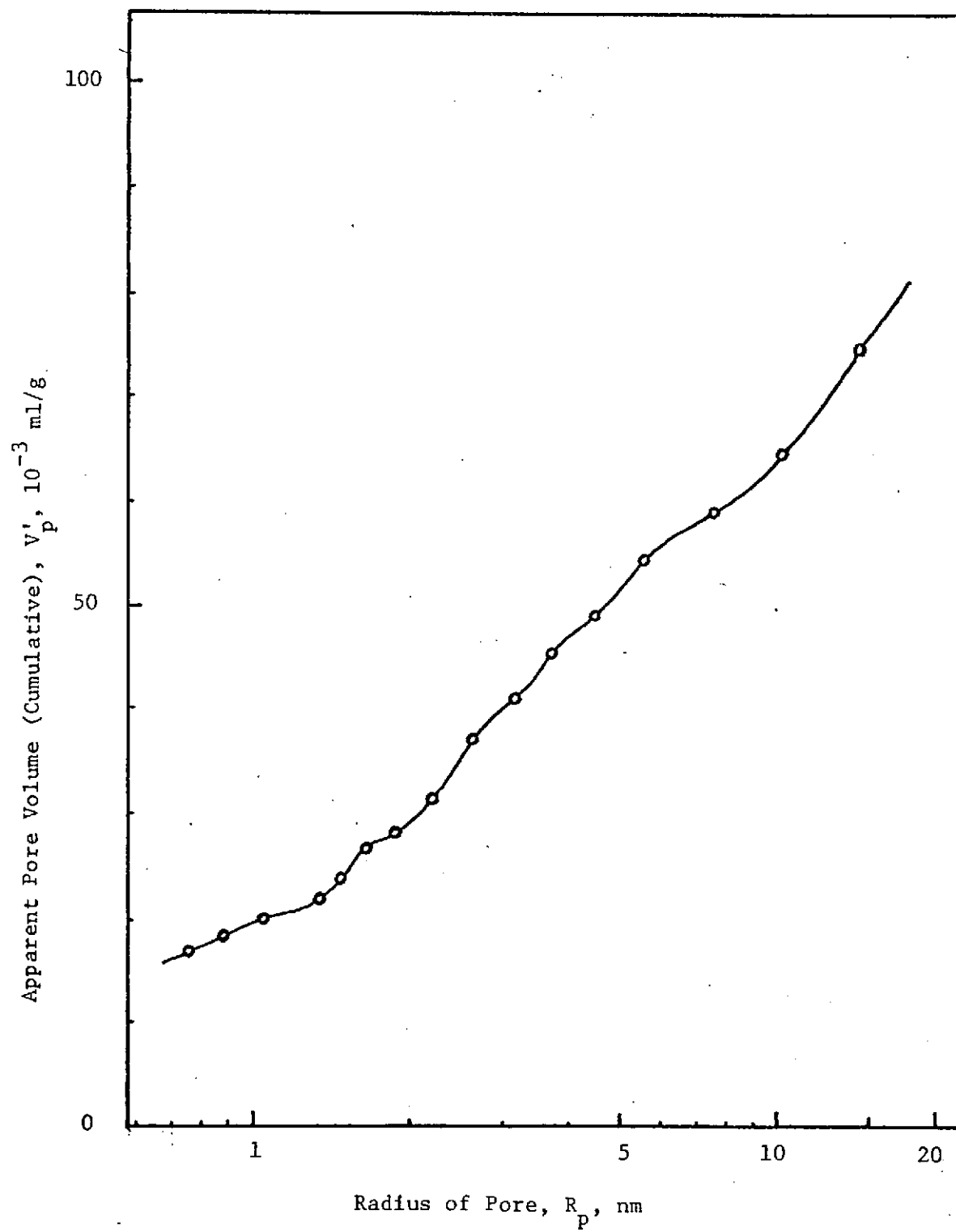


Figure 2: Pore Size Distribution of Asbestos-2

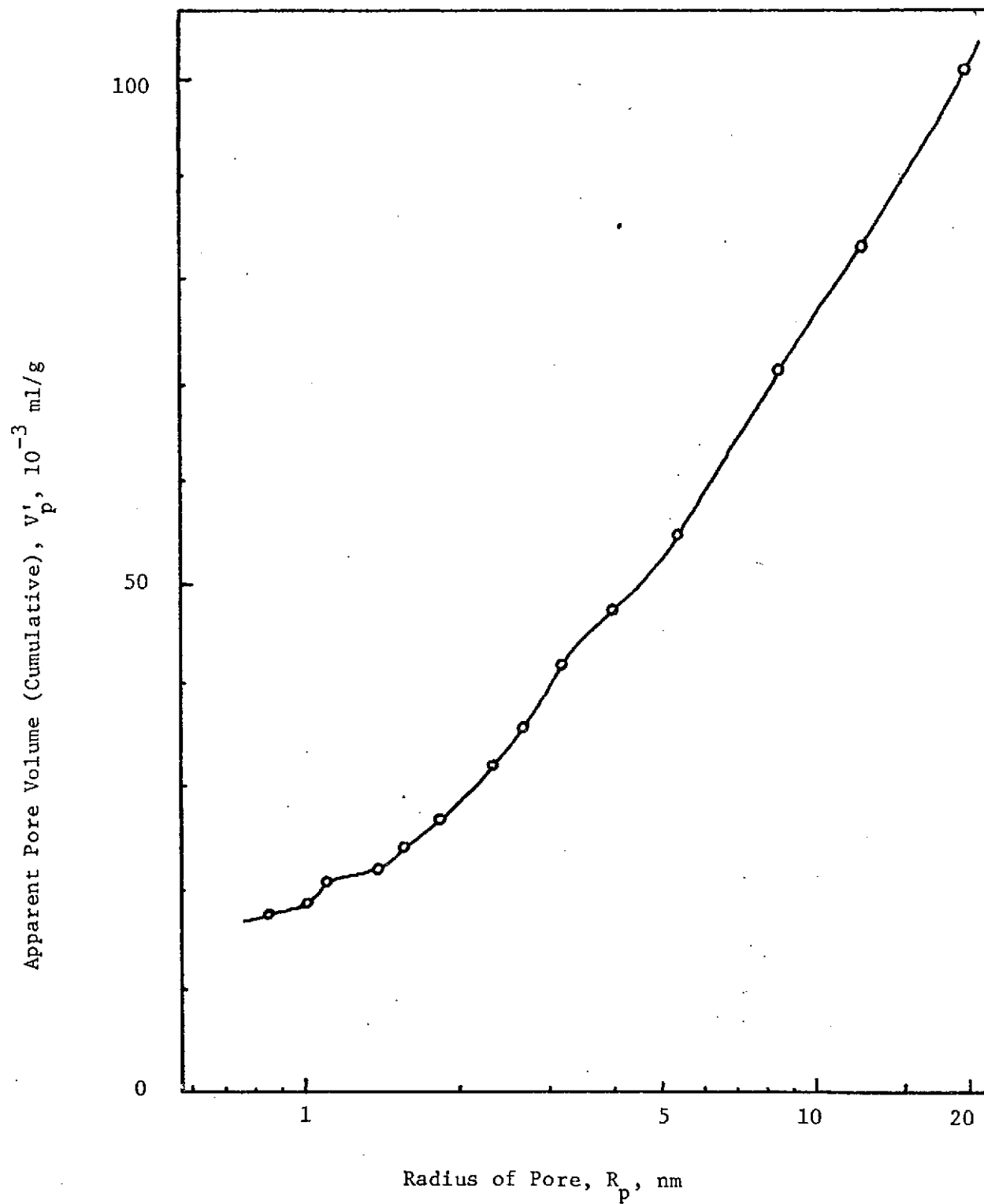


Figure 3: Pore Size Distribution of Asbestos-3

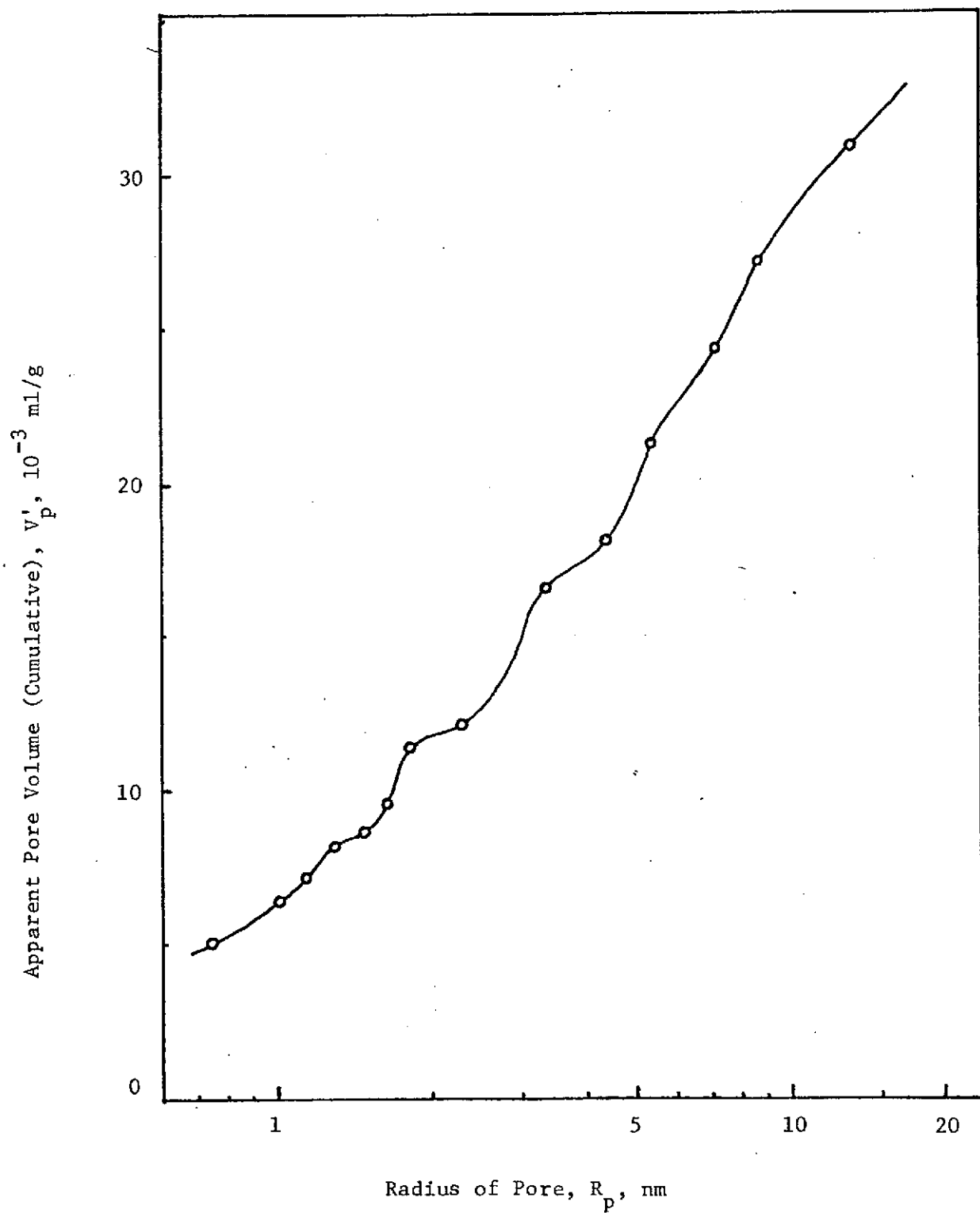


Figure 4: Pore Size Distribution of Fybex-1

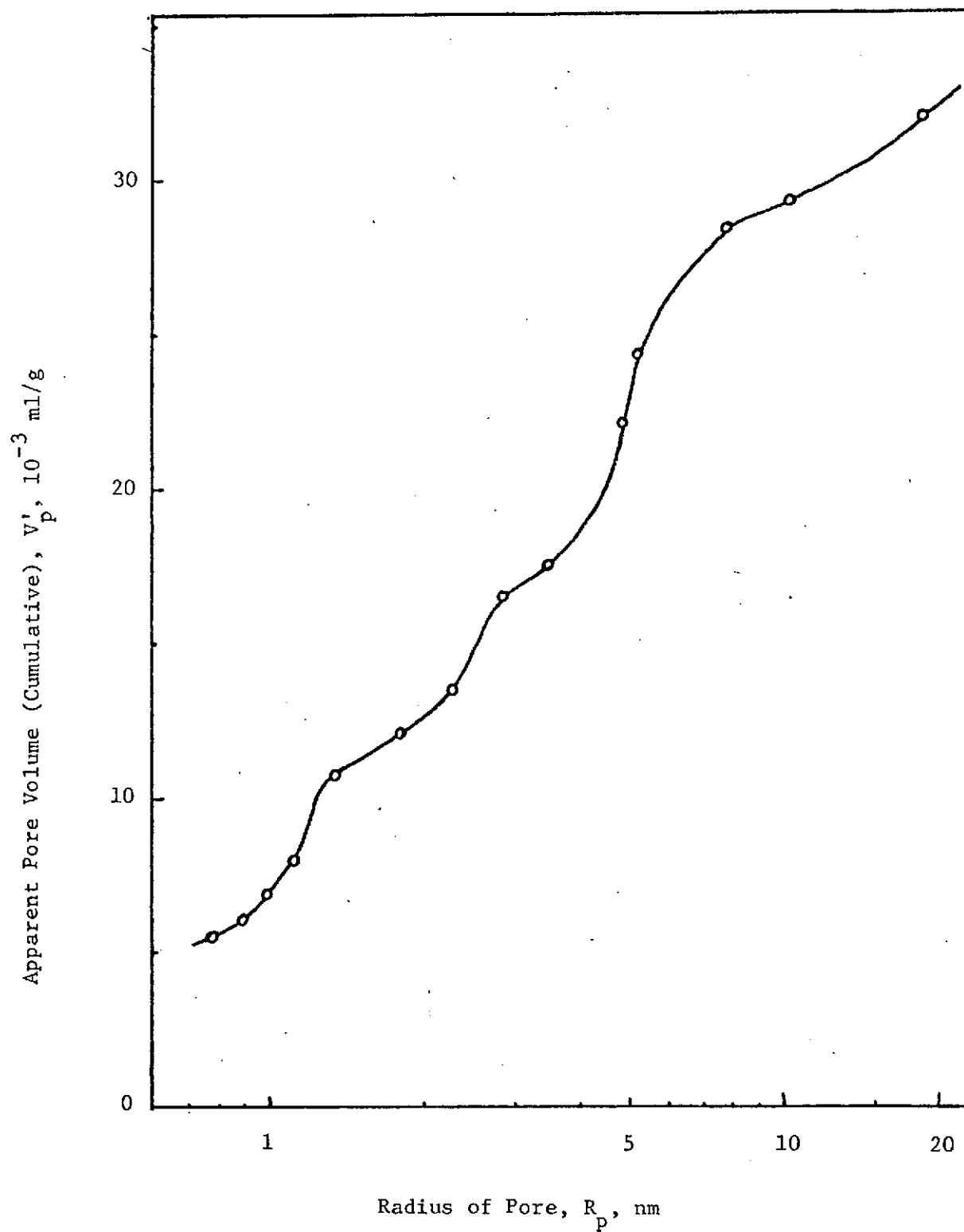


Figure 5: Pore Size Distribution of Fybex-2

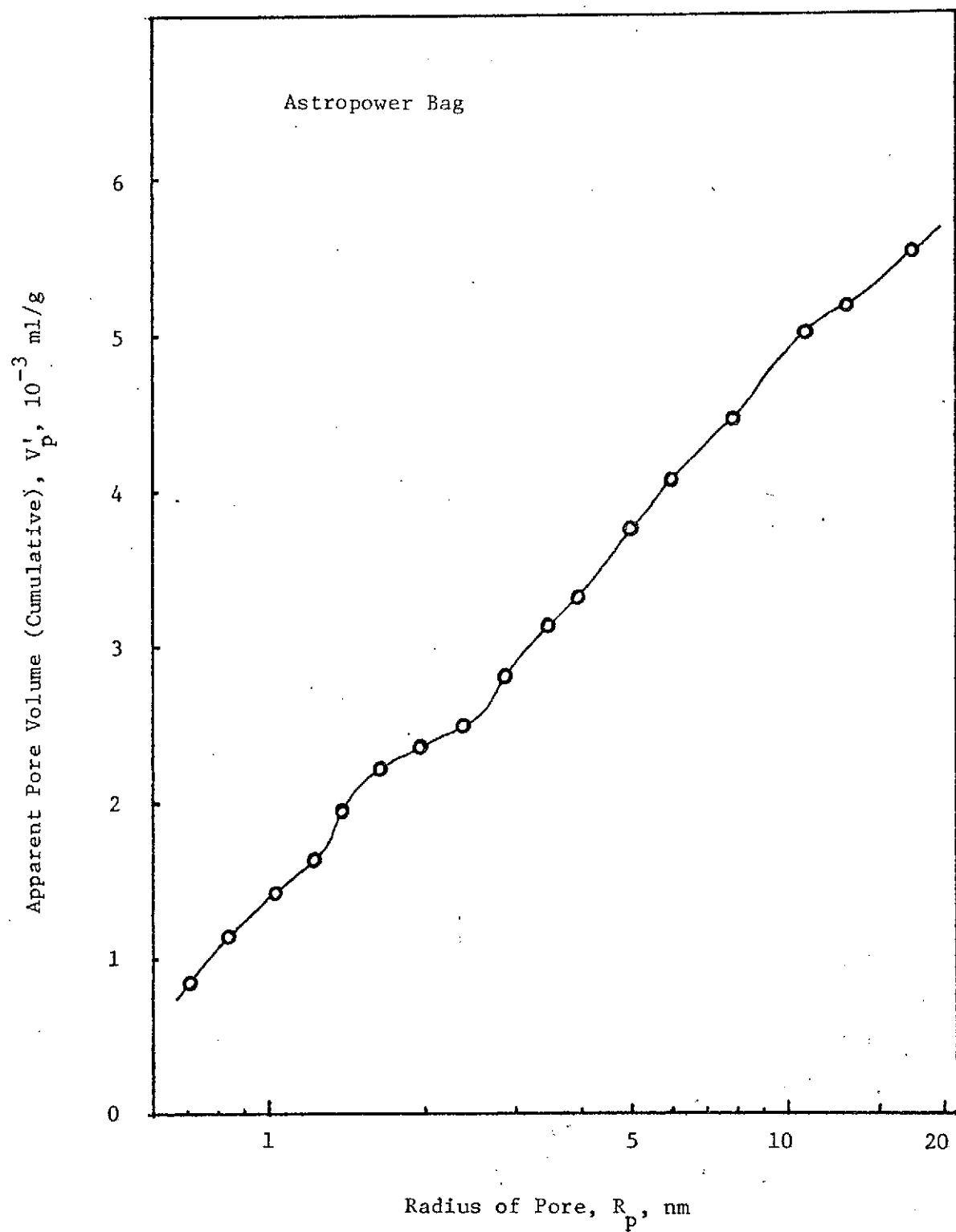


Figure 6: Pore Size Distribution of Astropower Bag

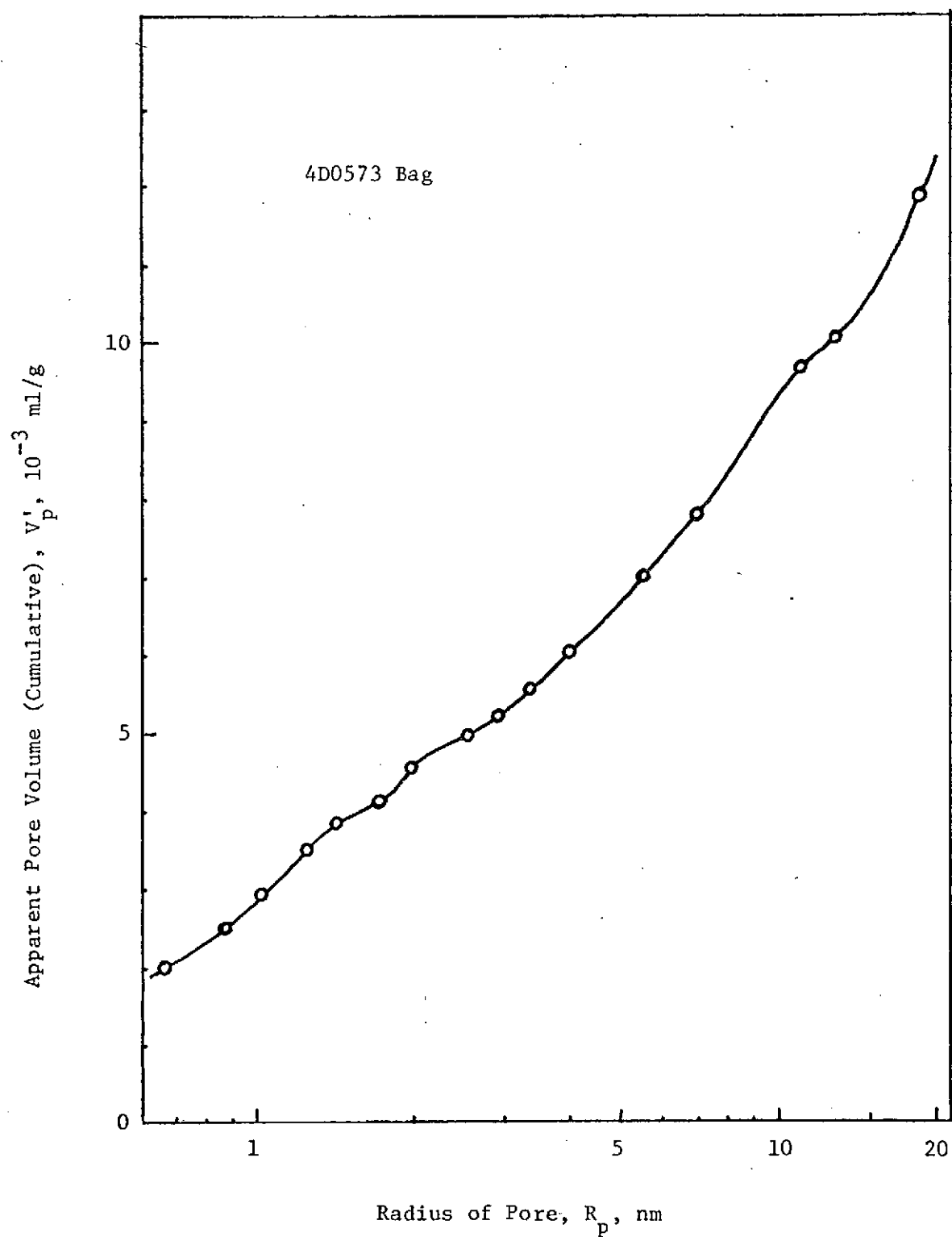


Figure 7: Pore Size Distribution of 4D0573 Bag



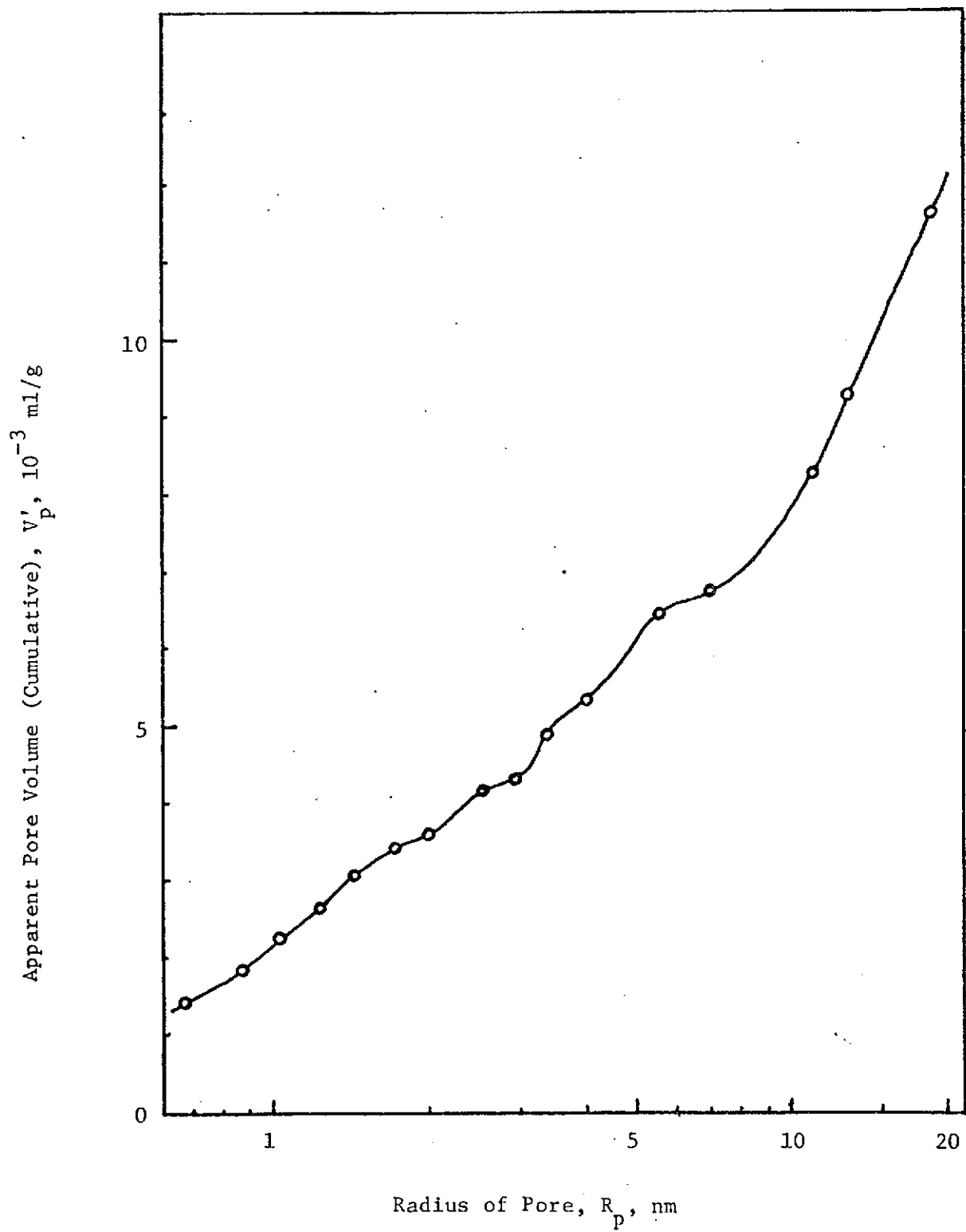


Figure 8: Pore Size Distribution of 4D0573 Sheet

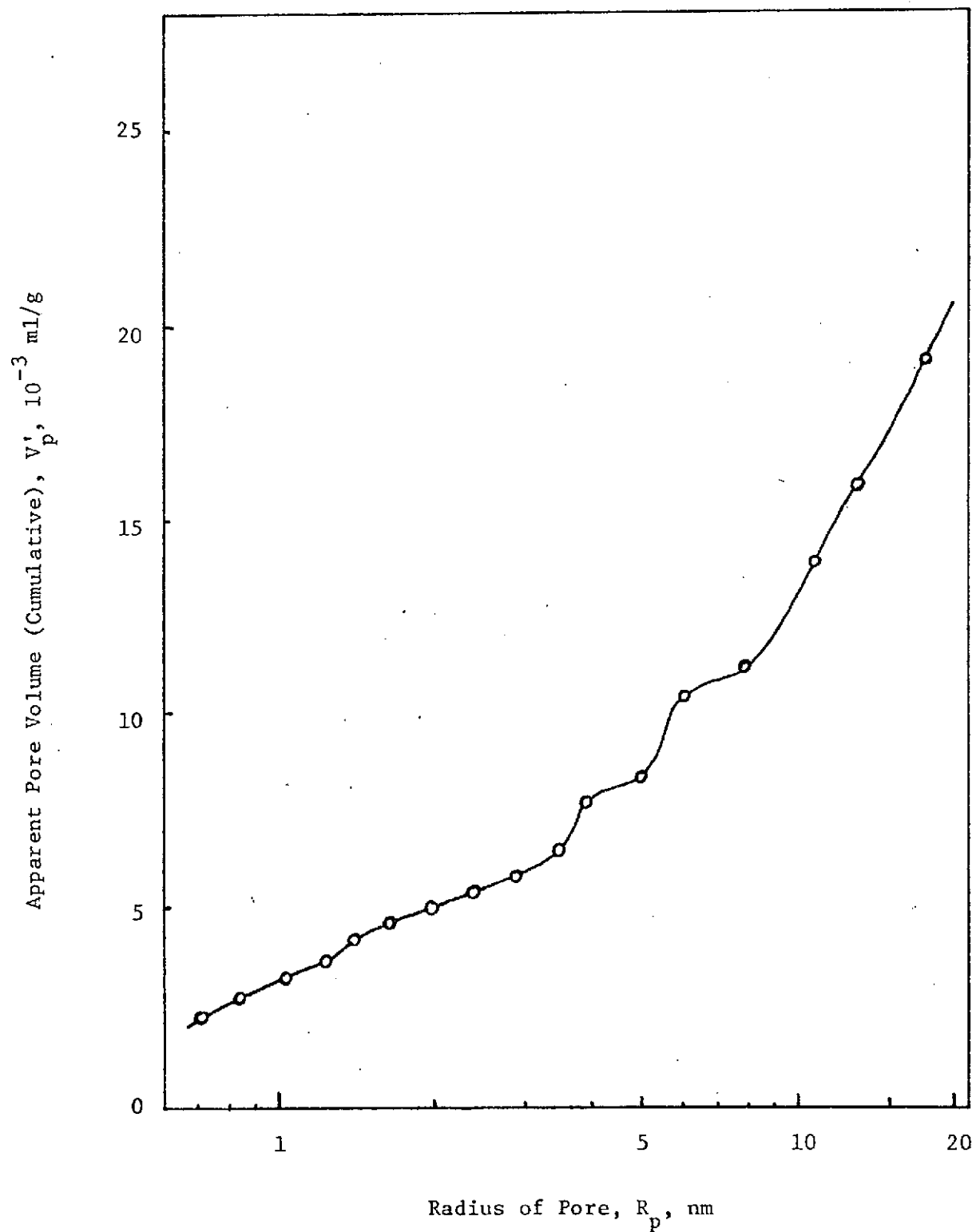


Figure 9: Pore Size Distribution of 11D2172 Sheet

Table 2.1

Surface Area and Pore Volume  
of Electrolyte Matrix Materials

	<u>Surface Area</u>	<u>Apparent Pore Volume</u>
	$\frac{\text{m}^2}{\text{g}}$	$\frac{\text{ml}}{\text{g}}$
Asbestos-1	44.3	0.148
Asbestos-2	44.4	0.155
Asbestos-3	44.0	0.227
Fybex-1	15.7	0.0357
Fybex-2	16.7	0.0666
4D0573 Sheet	5.5	0.0186
4D0573 Bag	7.1	0.0233
Astropower Bag	3.9	0.0214
11D2172 Sheet	7.9	0.0225

Table 2.2

Preferred Pore Sized In Electrolyte Matrix Samples

<u>Sample</u>	<u>Pore Radius, <math>R_p</math>, nm</u>			
Asbestos-1	3.1,	5.5,	12.0	
Asbestos-2	1.5,	2.3,	10.0	
Asbestos-3	1.0,	2.5,	6.0	
Fybex-1	1.2,	1.7,	3.0,	5.0
Fybex-2	1.1,	2.5,	5.0	
4D0573 Sheet	2.2,	3.2,	9.0	
4D0573 Bag	1.8,	10.0,	15.0	
Astropower Bag	1.4,	2.5		
11D2172 Sheet	3.5,	5.5,	10.0	

Since there exists more than one population of pores, the computer program described in the Fifteenth Semi annual report was used in analyzing the pore size distribution data. In Table 2.3 the computer analysis for the asbestos and Fybex materials is given.

Table 2.3

Computer Analysis of Pore Size Distribution  
of Fuel Cell Electrolyte Matrix Materials

<u>Fybex-1</u>		<u>Fybex-2</u>	
<u>Local Maxima</u>	<u>Mean Radius &amp; Std. Dev.</u>	<u>Local Maxima</u>	<u>Mean Radius &amp; Std. Dev.</u>
1.2	1.1 $\pm$ 0.2	1.0	1.1 $\pm$ 0.2
1.7	1.7 $\pm$ 0.1		
3.0	2.8 $\pm$ 0.6	2.5	2.4 $\pm$ 0.4
5.0	5.1 $\pm$ 0.7	5.1	5.3 $\pm$ 2.0
7.7	8.6 $\pm$ 2.0		

<u>Asbestos-1</u>		<u>Asbestos-2</u>		<u>Asbestos-3</u>	
<u>Local Maxima</u>	<u>Mean Radius &amp; Std. Dev.</u>	<u>Local Maxima</u>	<u>Mean Radius &amp; Std. Dev.</u>	<u>Local Maxima</u>	<u>Mean Radius &amp; Std. Dev.</u>
0.8	0.8 $\pm$ 0.05	0.8	0.8 $\pm$ 0.04		
1.0	1.0 $\pm$ 0.07	1.1	1.1 $\pm$ 0.1	1.1	0.9 $\pm$ 0.2
1.4	1.8 $\pm$ 0.4	1.5	1.5 $\pm$ 0.1	1.5	1.6 $\pm$ 0.1
		1.9	2.0 $\pm$ 0.1		
		2.4	2.5 $\pm$ 0.2	2.5	2.6 $\pm$ 0.8
3.1	3.0 $\pm$ 0.2	3.3	5.3 $\pm$ 2.9		
4.7	5.4 $\pm$ 1.0			8.0	8.8 $\pm$ 4.7

From Figures 1, 2, and 3 we can see that the pore size distribution curves for the three samples of asbestos are very similar. Indeed, the differences in the graphs may be more indicative of the reproducibility

of the experimental measurements than of real differences between the samples.

Figures 4 and 5 indicate that Fybex forms sheets with similar preferred pore sizes to asbestos but that the surface area and cumulative pore volume are less than for asbestos because of the larger fiber size of Fybex.

The Astropower bag, the 4D0573 bag and sheet, and the 11D2172 sheet are all impregnated with polyphenylene oxide (PPO) and coated on one side with a suspension of zirconia (and perhaps other materials) in PPO. This results in a sharp reduction of the surface area and apparent pore volume (all of these samples have a basic framework of asbestos). The pore size distribution curves shown in Figures 6-9 reflect the changes in surface area and pore volume, but they also reflect some differences between the samples themselves. The cumulative pore volume of the Astropower sample is the highest of the group and the curve in Figure 6 reveals less structure than is the case for the other coated matrix samples. While the difference between samples is small, it does appear that the curve for the Astropower sample is significantly different from the others.

Since the Astropower sample is believed to represent a superior electrolyte matrix, it seems worth noting here that the pore size distributions in these samples appear to be different in the following respects: 1) the Astropower sample appears to have a larger number of pores of a given size than do any of the other samples, 2) the pore size distribution in the Astropower sample appears to be more uniform than that of the other samples as revealed by the smoothness of the cumulative pore volume versus pore radius plot. It will be seen

in the next section of this report that the asbestos bundles appear to be broken down more completely and that the range of particle sizes on the coated side is greater for the Astropower sample than is the case for the other samples. These observations appear to be consistent with those made here.

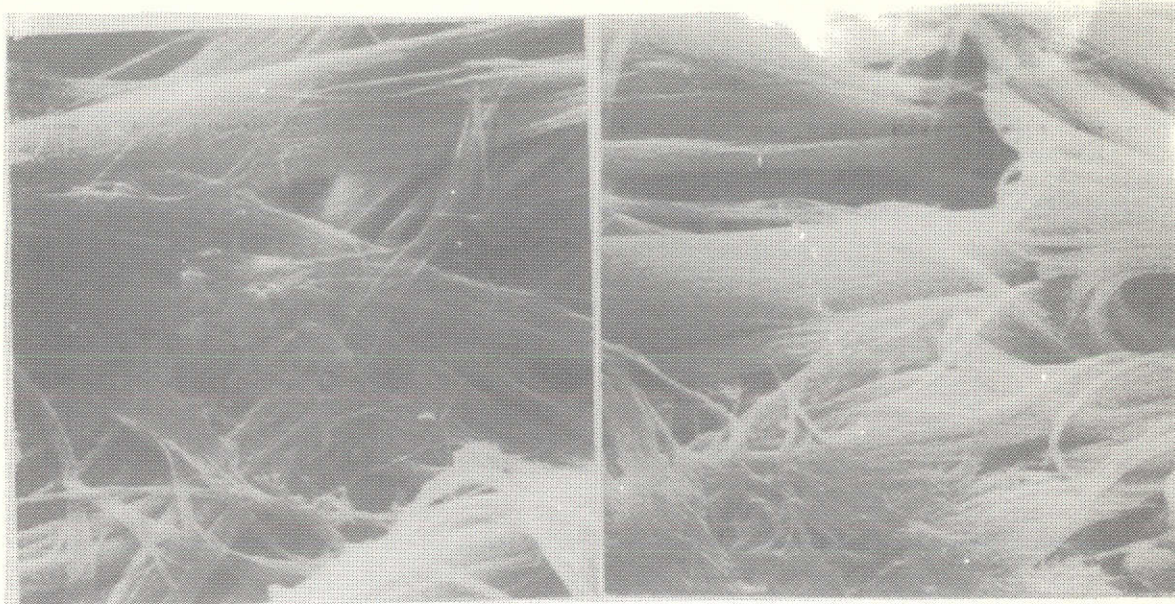
### 3. Electron Microscopy of Electrolyte Matrix Samples--M. C. Lee

As noted earlier the last four of the nine samples listed in Table 2.1 have been impregnated with polyphenylene oxide (PPO) and coated on one side with a slurry of zirconia in PPO. Scanning electron micrographs of both sides of these samples have been made, and some of these are shown in Figures 10 and 11.

In Figure 10 we see scanning electron micrographs of the uncoated side of the Astropower bag, the 4D0573 bag, the 4D0573 sheet, and the 11D2172 sheet all at 5000X magnification. Examination of these electron micrographs indicates that the asbestos bundles in the Astropower bag are more completely broken up than in the other matrix samples. In particular, the proportion of fibers of small radius is much larger in the Astropower sample than in the others.

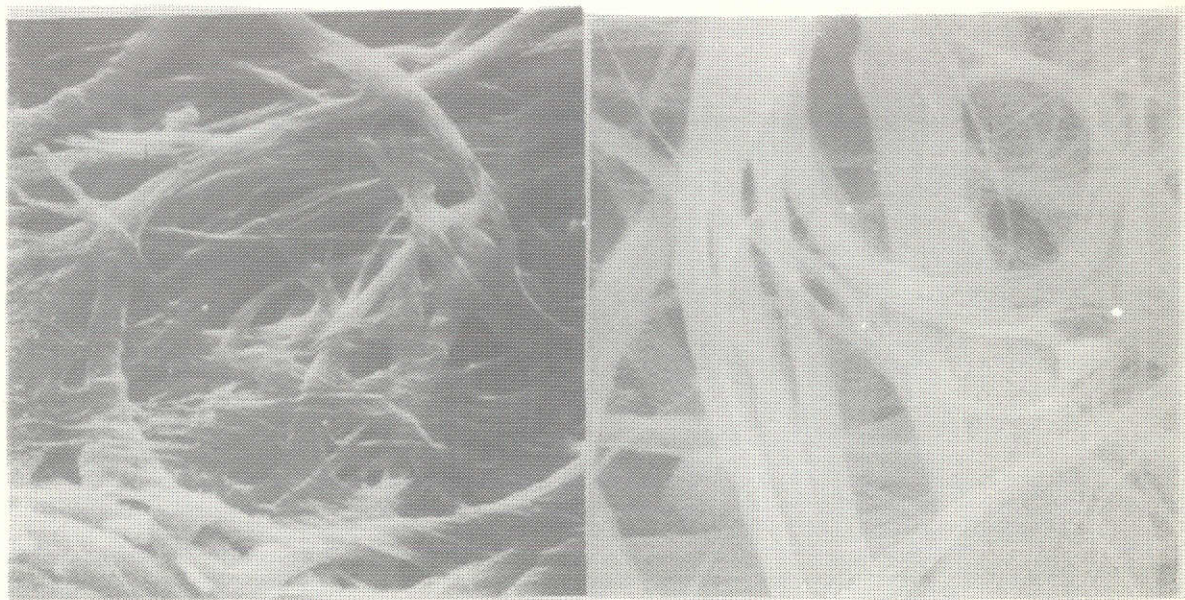
Scanning electron micrographs of the coated side of these samples are shown in Figure 11. Although the magnification is too low to reveal as much detail as is desired, the difference between the Astropower sample and the others is very obvious. Many large flat plates are on the surface of the Astropower sample but these plates show some evidence of being platelike aggregates of very much smaller crystallites. The larger plates appear to be 5-10 micrometers in length and perhaps one micrometer in thickness. Numerous smaller plates, one to a few micrometers in length, appear. In contrast, the other electrolyte matrices appear to contain more uniformly sized particles of a micrometer or so in size, little evidence of a platelike character, and an apparently lower concentration of powder in the coating.





4D0573 Bag

4D0573 Sheet

Astropower Bag  
Inside

11D2172 Sheet

This page is reproduced at the back of the report by a different reproduction method to provide better detail.

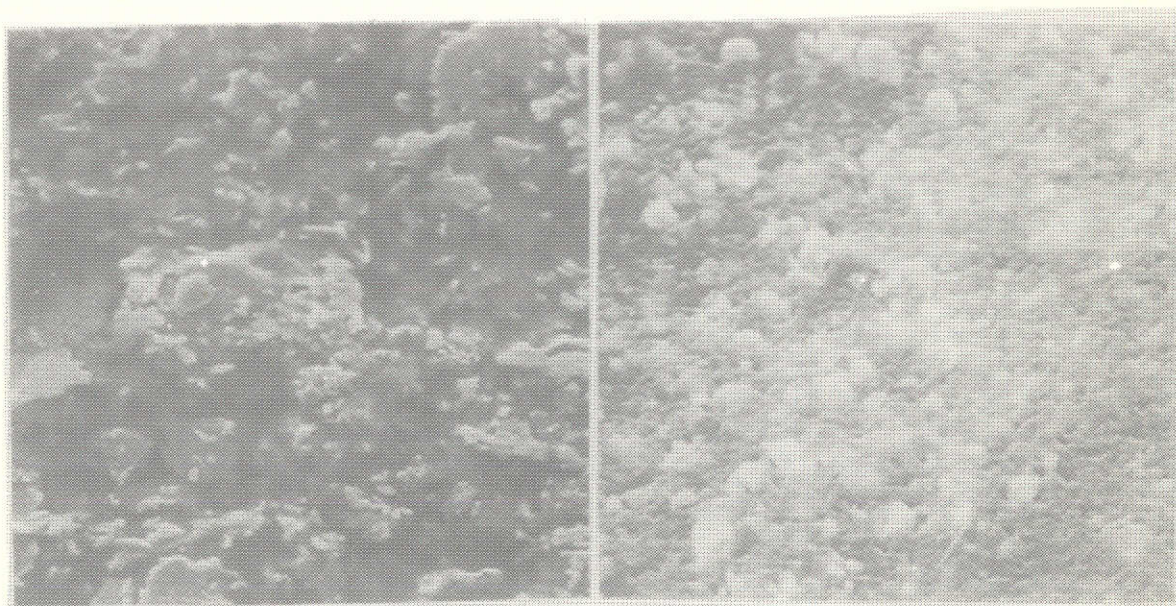
Figure 10. Scanning Micrograph of Uncoated Side of Electrolyte Matrices. 5000 X





4D0573 Bag  
Skin Side

4D0573 Sheet  
Skin Side



Astropower Bag  
Skin Side

11D2172 Sheet

This page is reproduced at the back of the report by a different reproduction method to provide better detail.

Figure 11. Scanning Electron Micrographs of Coated Side of Electrolyte Matrices. 2000 X

Electron micrographs at higher magnification were attempted; unfortunately the resolution was poor and little or no information could be derived from them. This approach will be explored further in an effort to ascertain whether the plates in the Astropower matrix are porous, and to determine more of the size, shape, and character of the particles in the coating of the other matrices.

#### 4. Distribution and Movement of Electrolyte in Fuel Cells--H. Lathanh

##### 4.1 The Surface Tension of KOH Solutions

In studying the distribution and movement of electrolyte inside porous structures it is useful to know the magnitude of the surface tension of the electrolyte and its dependence on solute concentration and temperature. The surface tension of KOH solutions at different concentrations has been measured at room temperature, and a search of the literature has revealed a recent extensive investigation by Feldkamp (1) for a wide range of temperatures and KOH concentrations, with which our experimental measurements agree well at the concentrations of interest.

In this section of the report we shall discuss our own measurements, and then we shall deal with those of Feldkamp and other investigators.

##### 4.1.1 Experimental Methods--The Wilhelmy Plate Method

Measurements were made on KOH solution in laboratory atmosphere by the Wilhelmy plate method, using a surface tensiometer. The method consists of measuring the pull,  $W$ , of a liquid solution on a completely wettable vertical plate of perimeter,  $p$ , and the surface tension is calculated from

$$\sigma \frac{\text{dynes}}{\text{cm}} = \frac{W \text{ dynes}}{p \text{ cm}} \quad (4.1-1)$$

This method is only moderately accurate owing to the difficulty in positioning the plate very precisely so as to eliminate buoyancy forces, and to the presence of a supermeniscus film whose thickness and

density depend on the solute concentration. The force  $W$  is measured by a torsion spring, but it was preferable in our case to calibrate the apparatus using pure water for which the surface tension is known with high accuracy (2).

#### 4.1.2 Preparation of Solutions

Reagent-grade potassium hydroxide pellets were used to prepare KOH solutions of concentrations up to saturation. The methods of preparation varied. In the most careful runs, the following procedure was used:

Wash five 250 ml glass beakers with soap and water; carefully rinse away all the soap.

Wash the beakers with concentrated nitric acid for a few seconds, rinse with de-ionized water, then with distilled water from a quartz still.

Allow to dry in laboratory atmosphere.

Repeat the procedure with five petri dishes which will serve as covers.

To the nearest milligram weigh KOH pellets directly into the 250 ml beakers to prepare 50 ml of the desired solution concentration. The concentrations are chosen to cover a suitable range, including zero concentration.

Add water slowly, with the beaker on the balance, to make the desired weight percent concentration within one percent.

Allow the system to cool in a water bath, until the desired temperature is reached with the Petri dish covers on to minimize evaporation.

Place the beaker on the balance again and add water to compensate for the amount evaporated, to the nearest centigram.



Cover the beakers, leave them in the bath again, and prepare the surface tensiometer by boiling the hanging plate in distilled water and then drying over a gas flame.

#### 4.1.3 Experimental Results

Measurements at 21 to 23°C on solutions ranging in concentration from 0.5 to 51 w/o yielded a total of 46 experimental points, of which only 12 were considered good. The surface tension for water was readily reproducible and did not differ for distilled or ordinary tap water. The surface tension values for KOH solutions, however, showed wide fluctuations which characteristically led to the following behavior:

- 1) The scatter in the data was larger for higher concentrations.
- 2) All values lay below a clearly defined upper boundary.
- 3) At the higher concentrations, the readings showed a rapid change with time, always decreasing when this occurred.

These observations point to the presence of some surface active agent in the test solutions, whose effect was dramatized by the high concentration of electrolyte, considering that high-concentration solutions had a propensity to exhibit much depressed surface tension values, at times far lower than that of water. When this did not happen, the "good" data lay on the upper boundary, and were considered to represent the true values of the surface tension of KOH. These data are listed in Table 4.1. Although the precision of the measurements was about 1%, the accuracy is lower for the reasons mentioned. Figure 12 shows a comparison of the experimental data with values reported by Faust (3) at 18°C and the correlation of Feldkamp (1) at 20°C, all set on a scale relative to water.

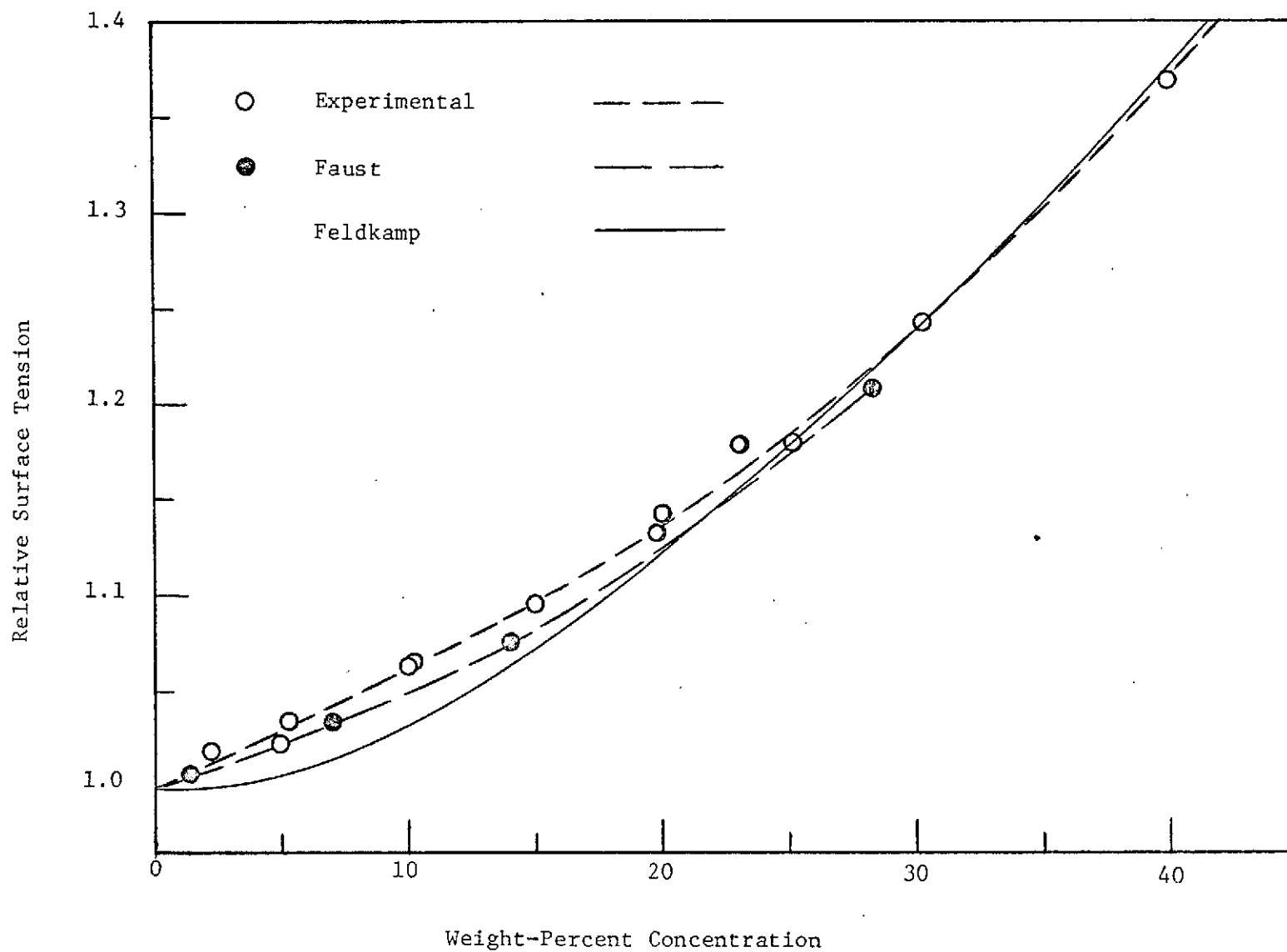


Figure 12: Surface Tension of KOH Solutions

Table 4.1

## Surface Tension of KOH Solutions

$$T = 21 - 23^{\circ}\text{C}$$

Concentration w/o	$\sigma$ dynes/cm	$\sigma/\sigma_o$
0	72.5	1.000
2.2	73.8	1.018
5.0	74.1	1.022
5.3	74.9	1.033
10.0	77.0	1.062
10.2	77.1	1.064
15.0	79.3	1.094
19.8	82.1	1.132
20.0	82.7	1.141
23.0	85.4	1.178
25.2	85.5	1.179
30.3	90.1	1.242
40.0	99.3	1.369

At the lower concentrations, the experimental data are higher than Faust's by 1% and the curve from Feldkamp is lower by 2%. However, for concentrations above 25 w/o, the curves show good agreement. Data from the International Critical Tables (2) along with some others between 15°C and 18°C were plotted in Figure 15 of our previous report (4). These agree with Faust's at concentrations below 10 w/o but diverge at

higher KOH concentrations. Their range is, however, limited to 17 w/o making them of limited importance for fuel cell electrolytes. The three sets of values shown in Figure 12 have each been correlated with a second-degree equation in concentration:

$$\sigma/\sigma_o = B_1 + B_2m + B_3m^2$$

where:  $\sigma$  = surface tension of solution, dynes/cm

$\sigma_o$  = surface tension of water at the same temperature, dynes/cm

$m$  = KOH concentration, w/o

Values of the coefficients and the closeness of fit are listed in Table 4.2.

Table 4.2-a

Coefficients of the Correlations:

$$\sigma = B_1 + B_2m + B_3m^2$$

	<u>Experimental</u>	<u>Faust</u>	<u>Feldkamp</u>
$B_1$	1.0035	0.9995	0.9988
$B_2$	0.004406	0.003135	0.00231
$B_3$	0.0001170	0.0001408	0.0001768
Goodness of Fit	0.40%	0.08%	0.53%
Concentration Range	40 w/o	28 w/o	60 w/o
Temperature	21-23°C	18°C	20°C



Table 4.2-b

Values Given by the Correlations

<u>m, w/o</u>	<u>Experimental</u>	<u>Faust</u>	<u>Feldkamp</u>	<u>Agreement</u>
20	1.138	1.119	1.116	2.0%
30	1.241	1.220	1.227	1.7%
40	1.367	1.350	1.374	1.8%
50	1.516	1.508	1.556	3.2%

4.1.4 The Data of Feldkamp

Feldkamp (1) has made the most extensive measurements of the surface tension of KOH solutions for concentrations up to 60 w/o and temperatures from 20°C to 170°C, using the method of maximum bubble pressure. His data, which we feel are worth reproducing here, were correlated to within 1% by the following equation:

$$\sigma(t, \xi) = \sum_{i=1}^5 \left( \sum_{k=1}^5 a_{ik} t^{k-1} \right) \xi^{i-1} \quad (4.1-2)$$

where:  $t$  = temperature, °C

$\xi$  = concentration, weight ratio of solute to solution

and  $a_{ik}$  is the matrix of coefficients given by Table 4.3.

Table 4.3

Matrix of Coefficients of the Feldkamp Equation  $a_{ik}$ 

i \ k	1	2	3	4	5
1	75.4787	-0.138489	$-0.336392 \times 10^{-3}$	$0.475362 \times 10^{-6}$	$-0.264479 \times 10^{-9}$
2	-32.8890	1.34382	$-0.910138 \times 10^{-2}$	$0.396124 \times 10^{-4}$	$-0.573565 \times 10^{-7}$
3	614.527	12.8736	0.104855	$-0.449076 \times 10^{-3}$	$0.651193 \times 10^{-6}$
4	-1455.06	39.8511	-0.344234	$0.144383 \times 10^{-2}$	$-0.207599 \times 10^{-5}$
5	1333.62	-38.3316	0.335129	$-0.137313 \times 10^{-2}$	$0.194911 \times 10^{-5}$

Feldkamp also gave an expression correlating the relative surface tension,  $\sigma/\sigma_0$ , with the reduced temperature and concentration, but the fit is poor at the lower temperatures.

Equation 4.1-2 is of the form:

$$\sigma(t, \xi) = A_1 + A_2\xi + A_3\xi^2 + A_4\xi^3 + A_5\xi^4 \quad (4.1-2)$$

where the coefficients are in turn fourth-degree polynomials in temperature. In spite of the complexity of this expression and its impracticality for hand calculations, it is not readily reducible owing to the equal importance of all terms at high temperatures. For convenience, Table 4.4 gives values of the coefficients of Equation 4.1-2 for different temperatures. Table 4.5 gives values of the surface tension which are plotted in Figures 13 and 14, emphasizing the concentration and temperature dependence, respectively. Figures 15 and 16 show in the same respect the behavior of the relative surface tension.

Table 4.4

Coefficients of the Feldkamp Equation

Temperature, °C	A <sub>1</sub>	A <sub>2</sub>	A <sub>3</sub>	A <sub>4</sub>	A <sub>5</sub>
10	74.061	-20.322	495.83	-1089.6	982.46
20	72.578	-9.3454	395.51	-789.51	690.37
30	71.034	0.25742	311.09	-532.04	449.79
40	69.431	8.6900	240.28	-324.70	253.67
50	67.771	16.142	180.92	-155.60	95.404
60	66.058	22.788	131.03	-18.274	-31.147
70	64.293	28.792	88.766	93.159	-131.65
80	62.479	34.300	52.457	184.14	-211.29
90	60.619	39.448	20.577	259.59	-274.81
100	58.715	44.356	-8.2401	323.94	-326.47
110	56.769	49.131	-35.203	381.12	-370.06
120	54.783	53.866	-61.365	434.56	-408.92
130	52.759	58.641	-87.625	487.20	-445.89
140	50.700	63.521	-114.72	541.46	-483.37
150	48.607	68.558	-143.24	599.29	-523.29
160	46.483	73.790	-173.61	662.13	-567.10
170	44.328	79.242	-206.10	730.91	-615.79

Table 4.5

Surface Tension of KOH Data From Feldkamp

Temperature °C	Concentration, w/o						
	0	10	20	30	40	50	60
10	74.06	76.00	82.69	91.13	100.7	113.1	132.4
20	72.58	74.88	81.36	89.78	99.59	111.9	129.4
30	71.03	73.68	80.00	88.39	98.38	110.5	126.6
40	69.43	72.40	78.59	86.95	97.06	109.1	123.9
50	67.77	71.05	77.14	85.47	95.66	107.6	121.3
60	66.06	69.63	75.66	83.94	94.17	106.0	118.9
70	64.29	68.14	74.14	82.37	92.60	104.3	116.6
80	62.48	66.60	72.57	80.75	90.97	102.6	114.3
90	60.62	65.01	70.97	79.09	89.27	100.8	112.2
100	58.71	63.36	69.33	77.38	87.51	98.92	110.0
110	56.77	61.67	67.64	75.63	85.71	97.04	107.9
120	54.78	59.95	65.92	73.84	83.85	95.14	105.9
130	52.76	58.19	64.17	72.08	81.96	93.21	103.8
140	50.70	56.40	62.37	70.14	80.03	91.25	101.8
150	48.61	54.58	60.55	68.22	78.07	89.28	99.80
160	46.48	52.73	58.69	66.28	76.08	87.30	97.78
170	44.33	50.86	56.79	64.30	74.06	85.30	95.75

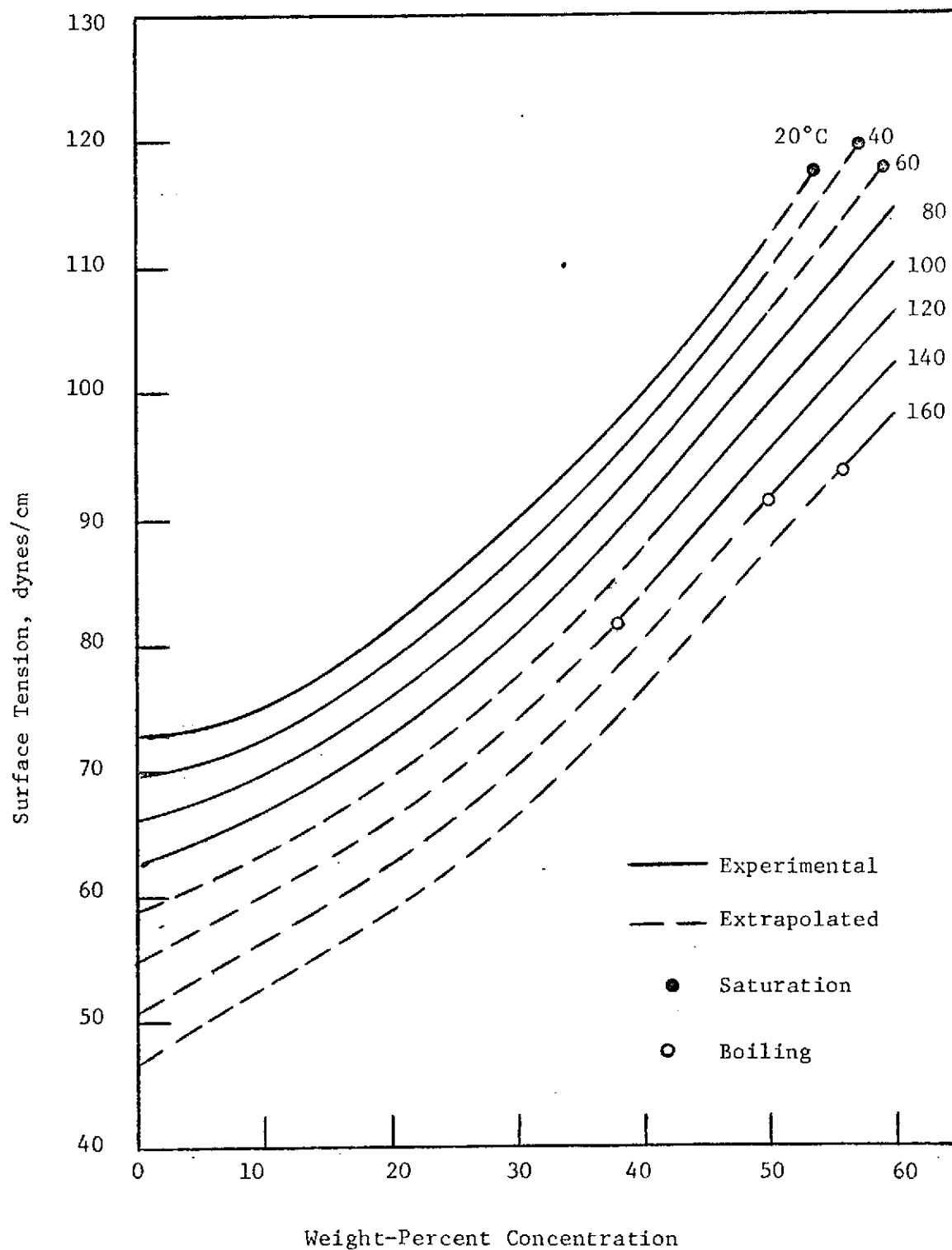


Figure 13: Surface Tension of KOH--Concentration Dependence  
 (Data From Feldkamp)

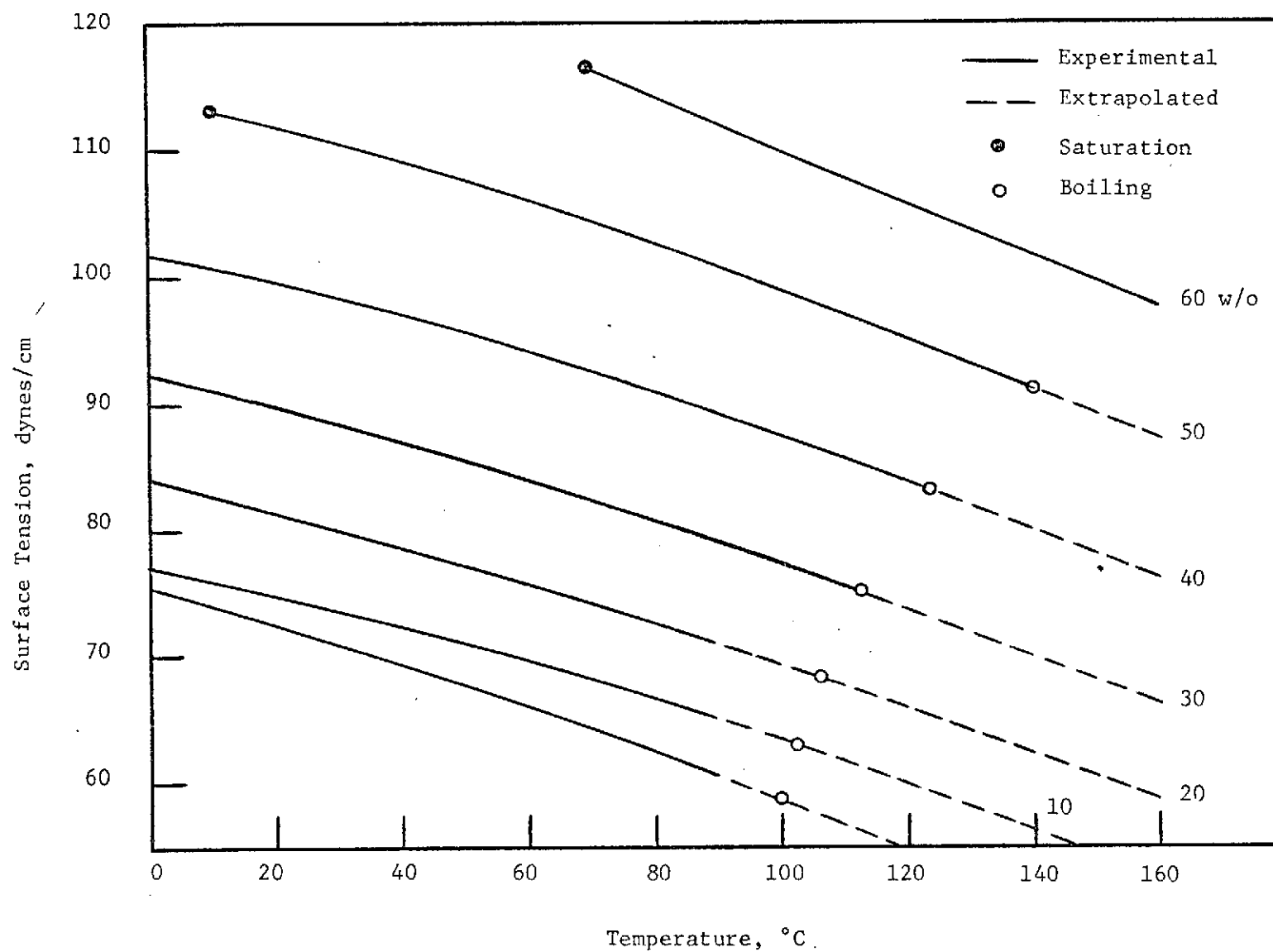


Figure 14; Surface Tension of KOH--Temperature Dependence  
(Data From Feldkamp)

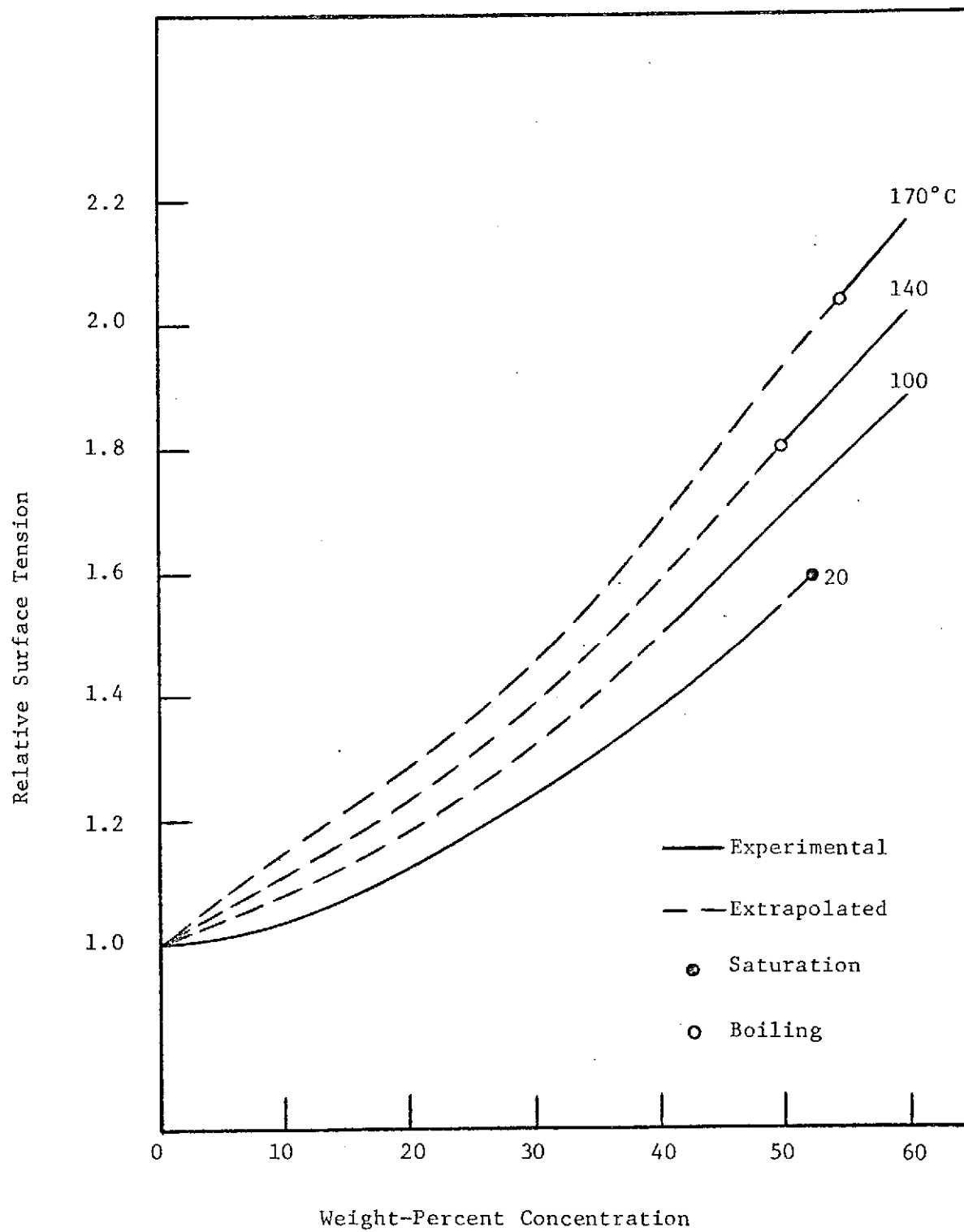


Figure 15: Relative Surface Tension of KOH-  
Concentration Dependence (Data From Feldkamp)



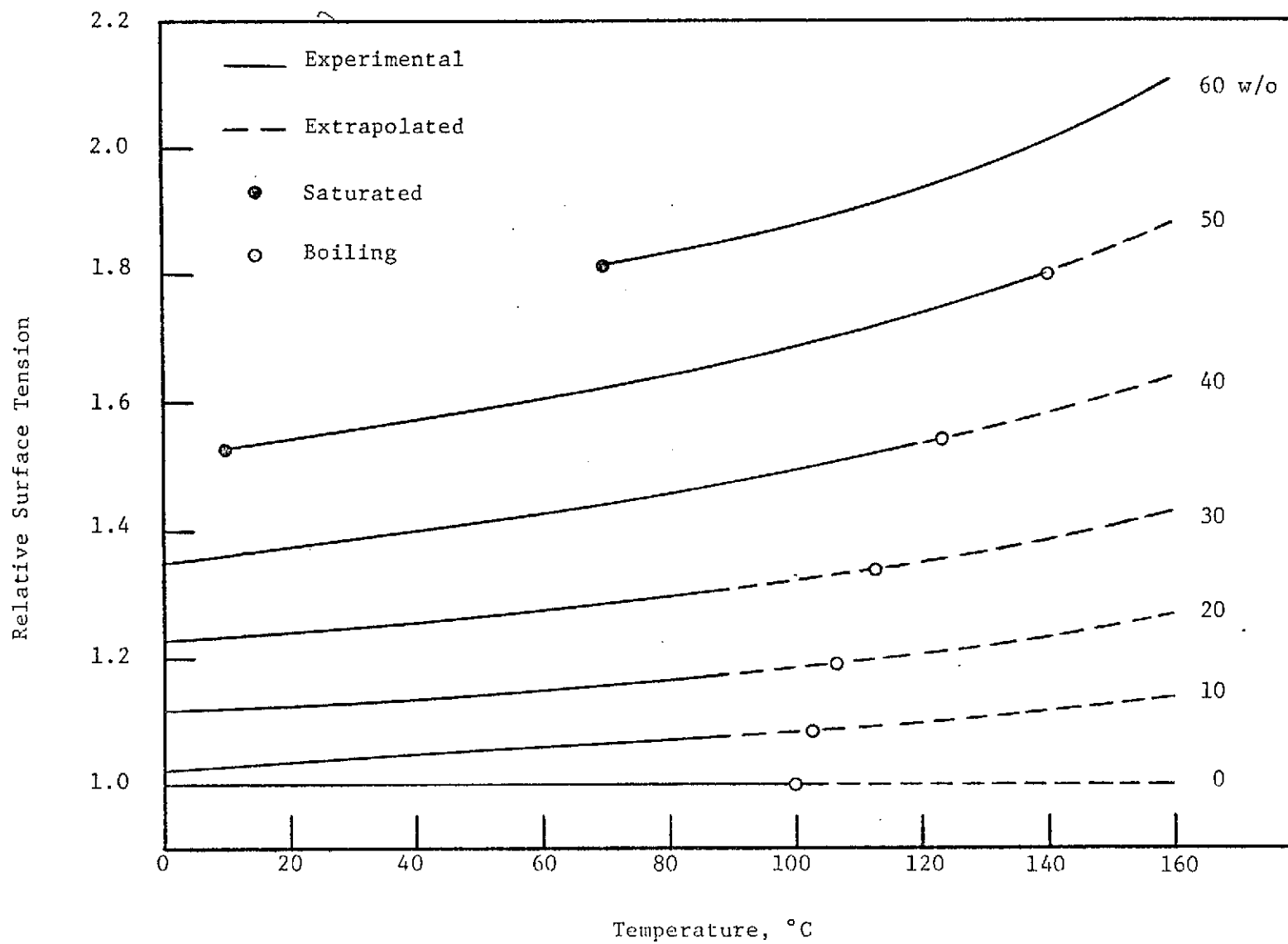


Figure 16: Relative Surface Tension of KOH--Temperature Dependence  
(Data From Feldkamp)

#### 4.1.5 Discussion

The agreement between the experimental data and those of Faust and Feldkamp bears out the reliability of the former. It is important to realize, however, that these represent the ideal situation of pure KOH solutions meticulously prepared and measured in an inert atmosphere (1). Our observations tend to show that, in many instances, the measured values of surface tension are much lower than the expected values, and that the difference is greater at the higher concentrations. Since the test solutions were prepared carefully, it is likely that the surface active agents were present in the laboratory atmosphere and slowly adsorbed onto them. If such is the case, then either the presence of ions in the solutions greatly enhances the effect of these agents, or it facilitates their adsorption, or both. Until the agents and effects are identified and quantified, there is little point in knowing precisely the surface tension of KOH under ideal conditions. It is likely that in mass-produced fuel cells operating for long times, the organic structural materials pollute to a certain degree the electrolyte solution, and that this alters its surface tension very significantly. It is thus important to evaluate the effect of these pollutants and that of carbon dioxide on the surface tension. It is also important to determine the dependence on surface tension of the overall cell performance.

#### 4.2 Modelling of Wetting and Penetration of Porous, Heterogeneous Media

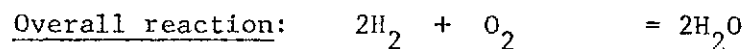
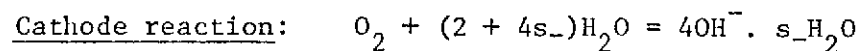
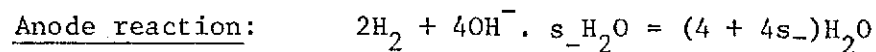
Literature and analytical studies of wetting in several simple porous or heterogeneous media are in progress but these have not yet led to definitive results. They will be described in a later report.

## 5. Water Transport In Alkaline H<sub>2</sub>-O<sub>2</sub> Fuel Cells--S. P. Lui

### 5.1 Introduction

Alkaline fuel cells, as pointed out by Kordesch (5), are technologically the most advanced fuel cell type today. Despite their high power output and increasingly lower cost, many problems remain to be solved before they can have extensive commercial applications. The concentration gradients of electrolyte in the matrix of an operating fuel cell have been measured by Miller and Fornasar (6), and by Lundquist and Vogel (7). However, to the best of the author's knowledge, the transport of free water within the electrolyte matrix has not been discussed in the literature. The principal objective of the present work is to look into the problem of water transport in the electrolyte matrix and to develop ways of estimating the concentration gradients of free water and the electrolyte in the matrix.

The overall reaction product in the alkaline H<sub>2</sub>-O<sub>2</sub> fuel cell is water. Water generated by this reaction must be removed from the cell to avoid dilution of the electrolyte, but water transport within the fuel cell is also very important in another sense: it is both a reactant at the cathode and a solvator of the hydroxyl ions formed there. The reactions at the electrodes can be written as follows:



where  $s_-$  is the primary hydration number of the hydroxyl ion.

It can be seen, then, that water must be transferred to the cathode both to maintain the cathode reaction and to solvate the hydroxyl ions produced there. It seems important to note here that water transport from the anode to the cathode involves transport of solvent water whereas water transport from the cathode to the anode involves transport of hydrated hydroxyl ions.

All of the ions in the electrolyte are hydrated but our principal concern is with the hydroxyl ions as these carry most of the intra-cell current and they participate in the electrode reactions, whereas potassium ions do not. As pointed out by Bockris (8), water may be regarded as being bound to ions in two ways: (1) strongly bound and (2) weakly bound. Strongly bound water--called the primary hydration sheath--is held so strongly to the ion that it moves with the ion. Weakly bound water--called the secondary hydration sheath--is attached so loosely to the ions that it behaves like a diffuse cloud around the ion and is in continuous interchange with water in the surrounding medium. We shall consider only the primary hydration sheath here. The number of water molecules in the primary hydration sheath of an ion is called the primary hydration number of the ion.

## 5.2 Mass Transfer in the Electrolyte Matrix

As we have seen earlier, transport processes in fuel cells are very important. In the following treatment mass transfer in the electrolyte matrix is considered. The electrolyte matrix usually consists of a thin sheet of specially processed asbestos with the voids between the asbestos fibers being filled with electrolyte, which, in our

case, is concentrated potassium hydroxide. We are able to deal with transport in this fuel cell component in a fairly rigorous manner because no chemical reactions occur in the electrolyte matrix. All transport takes place in the electrolyte solution which has three constituents: water, potassium, and hydroxyl ions. However, these ions do not exist as bare ions; rather, they exist as solvated ions and the water in the primary hydration sheath around the ion is fairly tightly bound so that it moves with the ion on the average. The equation of continuity for each species in the solution is given by

$$\frac{\partial c_i}{\partial t} = -\nabla \cdot N_i + R_i \quad (5.2-1)$$

where  $N_i$  is the flux of species  $i$ , expressed in moles/cm<sup>2</sup>-sec, and  $R_i$  is the rate of production of species  $i$  by chemical reaction expressed in moles/cm<sup>3</sup>-sec. Since no chemical reactions occur in the electrolyte matrix,  $R_i$  is zero, and since the electrolyte matrix is normally very thin, we need consider one-dimensional transport only. Therefore, at steady state Equation 5.2-1 becomes

$$\frac{dN_i}{dx} = 0$$

or

$$N_i = \text{constant} \quad (5.2-2)$$

In a multicomponent system, the momentum flux depends only upon the velocity gradients and the energy flux depends upon the temperature gradient. In the electrolyte matrix considered, although there may be some local variations in temperature, the temperature differences across the matrix are small compared to the absolute temperature. Therefore

we shall assume constant temperature in the electrolyte matrix. Also, because the electrolyte is contained in the small void spaces of the electrolyte matrix, we shall assume convection to be absent, i.e., the bulk velocity of the fluid in the matrix is zero. Hence it is not necessary to consider the equations of motion and energy.

The mass or molar flux of a species depends both on mechanical driving forces (ordinary, pressure, and forced diffusion) and on thermal diffusion effects. The multicomponent diffusion equation is (9)

$$c_i \left( \nabla \mu_i + \bar{s}_i \nabla T - \frac{M_i}{\rho} \nabla p \right) = RT \sum_j \frac{c_i c_j}{c_T \mathcal{D}_{ij}} \left[ (v_j - v_i) + \left( \frac{D_j^T}{\rho_j} - \frac{D_i^T}{\rho_i} \right) \nabla \ln T \right] \quad (5.2-3)$$

where  $\mu_i$  = electrochemical potential of species  $i$ , J/mole;  
 $\bar{s}_i$  = partial entropy of species  $i$ , J/mole-deg;  
 $\mathcal{D}_{ij}$  = diffusion coefficient of  $i$  in  $j$ , cm<sup>2</sup>/sec;  
 $D_i^T$  = thermal diffusion coefficient of  $i$ , gm/cm-sec;  
 $c_T$  = total solution concentration, mole/l;  
 $v_i$  = average velocity of species  $i$ , cm/sec.

We have already assumed that the temperature in the electrolyte matrix is constant and the gradient of pressure is usually very small. Thus, the thermal diffusion and the pressure diffusion terms are usually of only secondary importance and may be neglected. Equation 5.2-3 then takes the form

$$c_i \nabla \mu_i = RT \sum_j \frac{c_i c_j}{c_T \mathcal{D}_{ij}} (v_j - v_i) \quad (5.2-4)$$

Equation 5.2-4 is the generalized form of the Stefan-Maxwell equation (10)..

The  $\mathcal{D}_{ij}$  are the diffusion coefficients describing the interactions between species i and j. These coefficients are a set of phenomenological coefficients and they follow the so-called "Onsager reciprocal relation", that is,

$$\mathcal{D}_{ij} = \mathcal{D}_{ji} \quad (5.2-5)$$

The term  $c_i \nabla \mu_i$  in Equation 5.2-4 is the driving force per unit volume acting on species i. For potassium hydroxide solutions we have two independent equations

$$c_+ \nabla \mu_+ = RT \left[ \frac{c_+ c_o}{c_T \mathcal{D}_{o+}} (v_o - v_+) + \frac{c_- c_+}{c_T \mathcal{D}_{-+}} (v_- - v_+) \right] \quad (5.2-6)$$

$$c_- \nabla \mu_- = RT \left[ \frac{c_- c_o}{c_T \mathcal{D}_{o-}} (v_o - v_-) + \frac{c_- c_+}{c_T \mathcal{D}_{-+}} (v_+ - v_-) \right] \quad (5.2-7)$$

where  $c_o$  = concentration of total water, moles/l;  
 $c_+$  = concentration of potassium ion, moles/l;  
 $c_-$  = concentration of hydroxyl ion, moles/l;  
 $c_T$  = total solution concentration, moles/l;  
 $\mu_+$  = electrochemical potential of the potassium ion;  
 $\mu_-$  = electrochemical potential of the hydroxyl ion.

The chemical potential of the electrolyte may be expressed as

$$\begin{aligned} \mu_e &= v_+ \mu_+ + v_- \mu_- \\ &= vRT \ln (c_{\pm} a_{\pm}^{\theta}) \end{aligned} \quad (5.2-8)$$

- where  $v_+$  = number of potassium ions produced by the dissociation of one molecule of potassium hydroxide;
- $v_-$  = number of hydroxyl ions produced by the dissociation of one molecule of potassium hydroxide;
- $v$  = number of moles of ions into which a mole of electrolyte dissociates;
- $f_{\pm}$  = mean molar activity coefficient of the electrolyte;
- $a_{\pm}^0$  = a constant of proportionality.

The number of moles of ions into which a mole of electrolyte dissociates,  $v$ , is given by

$$v = v_+ + v_- \quad (5.2-9)$$

The concentration of the electrolyte is defined by

$$c = \frac{c_+}{v_+} = \frac{c_-}{v_-} \quad (5.2-10)$$

The flux equations for the potassium ion and the hydroxyl ion may be obtained by rearranging Equations 5.2-6 and 7. For steady state conditions, these flux equations can be written as follows: (see Appendix 1 for details).

$$N_+ = c_+ v_+ = - \frac{v_+ D c_T c}{v R T c_o} \nabla \mu_e + \frac{i t_+}{z_+ F} + c_+ v_o \quad (5.2-11)$$

$$N_- = c_- v_- = - \frac{v_- D c_T c}{v R T c_o} \nabla \mu_e + \frac{i t_-}{z_- F} + c_- v_o \quad (5.2-12)$$

where  $D$  is the diffusion coefficient of the electrolyte and is given by

$$D = \frac{D_{o+} D_{o-} (z_+ - z_-)}{z_+ D_{o+} - z_- D_{o-}} \quad (5.2-13)$$



The transference numbers (with respect to the solvent velocity) are defined as follows

$$t_+ = 1 - t_- = \frac{z_+ \mathcal{D}_{o+}}{z_+ \mathcal{D}_{o+} - z_- \mathcal{D}_{o-}} \quad (5.2-14)$$

where we note that  $z_-$  has a negative value and the term  $-z_- \mathcal{D}_{o-}$  becomes positive. The measured diffusion coefficient,  $D$ , is related to  $\mathcal{D}$  by

$$D = \frac{\mathcal{D} c_T}{c_o} \left( 1 + \frac{d \ln \gamma_{\pm}}{d \ln m} \right) \quad (5.2-15)$$

where  $\gamma_{\pm}$  is the mean molal activity coefficient and  $m$  is the molality.

It can be shown that the relation between the gradient of chemical potential and the gradient of concentration is given by (see Appendix 2)

$$\frac{\mathcal{D} c_T c}{V R T c_o} \nabla \mu_e = D \left( 1 - \frac{d \ln c_o}{d \ln c} \right) \nabla c \quad (5.2-16)$$

Substituting Equation 5.2-16 into Equations 5.2-11 and 12, we get

$$N_+ = -v_+ D \left( 1 - \frac{d \ln c_o}{d \ln c} \right) \nabla c + \frac{it_+}{z_+ F} + c_+ v_o \quad (5.2-17)$$

and

$$N_- = -v_- D \left( 1 - \frac{d \ln c_o}{d \ln c} \right) \nabla c + \frac{it_-}{z_- F} + c_- v_o \quad (5.2-18)$$

For water, the total flux consists of the flux due to free water, that due to water of hydration, and that due to convection. Since potassium ions do not enter into the electrode reactions, the net flux of potassium ions is zero and the flux of hydration water with potassium ions is, therefore, zero. Thus, we have

$$N_{H_2O} = -D \frac{dc_{fw}}{dx} + s_- N_- + c_o v_o \quad (5.2-19)$$

where  $c_{fw}$  is the concentration of free water expressed in moles/l and  $s_-$  is the hydration number of the hydroxyl ion.

We have already assumed that convection is absent in the electrolyte matrix and that all transport is essentially one-dimensional, so the flux equations become

$$N_+ = -v_+ D \left( 1 - \frac{dlnc_o}{dlnc} \right) \frac{dc}{dx} + \frac{it_+}{z_+ F} \quad (5.2-20)$$

$$N_- = -v_- D \left( 1 - \frac{dlnc_o}{dlnc} \right) \frac{dc}{dx} + \frac{it_-}{z_- F} \quad (5.2-21)$$

$$N_{H_2O} = -D \frac{dc}{dx} fw + sN_- \quad (5.2-22)$$

In order to solve these equations, it is necessary to know the transference number and the hydration number of the ions. In the next two sections the transference number and the hydration number in concentrated potassium hydroxide solution will be discussed.

In Section 5.5 the concentration gradients for both the electrolyte and free water are calculated using both the transference number and the hydration number estimated for 30 w/o KOH.

### 5.3 Transference Numbers In KOH Solutions

The transference number of an ion,  $t_i$ , is the fraction of the total current carried by that ion, that is

$$t_i = \frac{i_i}{\sum_j i_j} \quad (5.3-1)$$

where  $i_i$  is the portion of current carried by the  $i$  species, expressed in  $\text{amp}/\text{cm}^2$ . Also, we note that

$$\sum_i t_i = 1 \quad (5.3-2)$$

Since the current density of an ion is proportional to the mobility of the ion, it can be shown that the transference numbers of the potassium and hydroxyl ions are given by

$$t_+ = \frac{u_+}{u_+ + u_-} \quad (5.3-3)$$

and

$$t_- = \frac{u_-}{u_+ + u_-} \quad (5.3-4)$$

where  $u_+$  and  $u_-$  are the mobilities of the potassium and hydroxyl ions, respectively, expressed in  $\text{cm}^2/\text{sec-volt}$ . The mobility of an ion in a solution is directly proportional to the conductance of the ion; hence transference numbers may also be expressed in the form

$$t_+ = 1 - t_- = \frac{\lambda_+}{\lambda_+ + \lambda_-} \quad (5.3-5)$$

where  $\lambda_+$  and  $\lambda_-$  are the ionic conductances of potassium and hydroxyl ions, respectively. The equivalent conductance of a binary electrolyte,  $\Lambda$ , is given by

$$\Lambda = \lambda_+ + \lambda_- \quad (5.3-6)$$

Hence,

$$t_+ = \frac{\lambda_+}{\Lambda} \quad (5.3-7)$$

Similarly, we have

$$t_- = \frac{\lambda_-}{\Lambda} \quad (5.3-8)$$

### 5.3.1 Methods for Measuring Transference Numbers

The chief methods for the determination of transference number are: the Hittorf method, the moving boundary method, and the electromotive force method.

### The Hittorf Method

This method is based on a procedure suggested by Hittorf in 1853 in which the transference number is determined by measuring the changes of concentration in a three-compartment cell in which a given current is passed through a solution of the electrolyte. This procedure is subject to many difficulties in practice, and accurate results are difficult to obtain. However, by using an improved apparatus, MacInnes and Dole (11), and Jones and Bradshaw (12) were able to obtain quite accurate results.

### The Moving Boundary Method

In the moving boundary method, the transference number is obtained by measuring the volume swept through by a boundary between two solutions during the passage of a given quantity of electricity. The transference number of the cation is given by

$$t_+ = \frac{FdAc^*}{Q} \quad (5.3-9)$$

where  $d$  = distance moved by the boundary, cm;

$A$  = cross-sectional area of the tube,  $\text{cm}^2$ ;

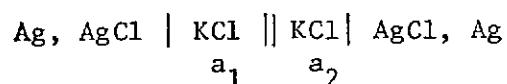
$c^*$  = concentration in equivalent per  $\text{cm}^3$ ;

$Q$  = quantity of electricity, coulomb.

For a detailed account of the theory and techniques of the moving boundary method, the reader is referred to MacInnes and Longworth (13). This method gives more accurate results than does the Hittorf method, and it is simpler experimentally.

### The emf Method

This method of measuring transference numbers is based on measurements of the emf of concentration cells with and without transference. A concentration cell with transference consists of two identical electrodes immersed in solutions of the same electrolyte having different compositions or solutions of different electrolytes having the same concentration. The difference in composition of the two solutions at their junction leads to diffusion and the development of a liquid junction potential. An example of a concentration cell with transference is

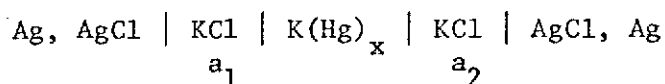


and the emf of the cell is given by

$$E_t = \pm t_{\pm} \frac{\nu RT}{\nu_{\pm} Z_{\pm} F} \ln \frac{a_2}{a_1} \quad (5.2-10)$$

where the subscript on E indicates that transference takes place, and  $a_1$  and  $a_2$  are the mean activities of the electrolyte in the left hand and right hand compartments of the cell.

A concentration cell without transference is one in which both electrodes are the same and immersed in the electrolytic solutions of different compositions but with no liquid junction between the anolyte and the catholyte. Since there is no liquid junction, ions cannot pass from one solution into the other. There is, therefore, no liquid junction potential in concentration cells without transference. An example of a concentration cell without transference is



where it is seen that the connection between the anolyte and the catholyte is a potassium amalgam. The emf of the cell is given by

$$E = \pm \frac{\nu RT}{\nu_{\pm} z_{\pm} F} \ln \frac{a_2}{a_1} \quad (5.3-11)$$

where  $\nu$  is the total number of ions, and  $\nu_+$  or  $\nu_-$  is the number of positive or negative ions produced by the dissociation of one molecule of electrolyte;  $z_+$  or  $z_-$  is the charge number of the positive or negative ions.

Since the difference in the emf of concentration cells with and without transference arises out of transference across the liquid junction, it follows, then, that we can determine the transference number by comparing the emfs of the respective cells. Thus, from Equations 5.3-10 and 11 we have

$$t_{\mp} = \frac{E_t}{E} \quad (5.3-12)$$

From Equations 5.3-7 and 8, the transference number of an ion is expressed as the ratio of the ionic conductance,  $\lambda_i$ , and the equivalent conductance of the solution,  $\Lambda$ , where the values of the conductances are those at the particular concentration of interest. Since the ionic conductances are concentration-dependent, it is not surprising to find that the transference number also vary with the concentration of the electrolyte.

Empirical equations for transference number as a function of concentration have been proposed by Jones and Dole (14), Longworth (15),

and Owen (16). These empirical equations give satisfactory results for aqueous solutions of 1-1 chlorides but the validity of these equations for potassium hydroxide solutions has not been tested adequately.

According to the Onsager equation the equivalent conductance of an ion,  $\lambda_i$ , is given by

$$\lambda_i = \lambda_i^0 - (1/2\alpha + \beta\lambda_i^0) \sqrt{c} \quad (5.3-13)$$

where  $\lambda_i^0$  is the ionic conductance of species  $i$  at infinite dilution, expressed in mho-cm<sup>2</sup>/eq,  $\alpha$  and  $\beta$  are constants. Thus, the transference number of the potassium ion is given by

$$t_+ = \frac{\lambda_+}{\lambda_+ + \lambda_-} = \frac{\lambda_+^0 - (1/2\alpha + \beta\lambda_+^0)\sqrt{c}}{\Lambda_0 - (\alpha + \beta\Lambda_0)\sqrt{c}} \quad (5.3-14)$$

For water as solvent,  $\alpha = 60.20$  and  $\beta = 0.229$ . The ionic conductances for the potassium and hydroxyl ions are 73.52 and 197.6 mho-cm<sup>2</sup>/eq, respectively. Using these values of the constants in Equation 5.3-14, values of the transference number for the potassium ion can be calculated.

Although dilute electrolytic solutions have been studied intensively, studies in concentrated electrolytic solutions have been less frequent; and while the Onsager theory predicts the concentration dependence of the transference number, it is applicable only at low concentrations. Attempts to extend the Onsager equation to higher concentrations have not met with success.

Recently, Merenkov (17) measured the transference number of potassium ion in KOH solutions from one equivalent to ten equivalents per liter. He found that the transference number of potassium ion was independent of

temperature from 18° to 65°C but that it decreased with increase in KOH concentration. The transference number of potassium ion was correlated by the empirical equation

$$t_+ = 0.26 - 0.047 (\sqrt{c} + 1) \quad (5.3-15)$$

On the other hand, Knobel (18) determined the transference number of the potassium ion in KOH solutions by the emf method; he found that the transference number of potassium ion was 0.2633 and that it was independent of concentration over the concentration range from 0.03N to 3.0N. The predictions of the Onsager equation and the experimental results of Knobel, and Merenkov are summarized in Table 5.1.

In fuel cell operations, we are dealing with concentrated solutions of KOH. The use of the Onsager equation certainly leads to erroneous results. The empirical equation proposed by Merenkov gives the concentration dependence of the transference number for concentrated solutions, yet it cannot be used for dilute solutions. The value at infinite dilution as predicted by Merenkov's empirical equation is 0.213, which is far below the theoretical value of 0.271. At a concentration of 1 N, however, the agreement between the Onsager and Merenkov equations is relatively good ( $t_{+O} = 0.176$  vs  $t_{+M} = 0.166$ ). It is clear that Knobel's data deviate from the Onsager equation very significantly when the potassium hydroxide concentration is greater than about 0.1 N.



Table 5.1

Summary of Transference Number Data for KOH Solutions

<u>Concentration of KOH Solutions (N)</u>	<u>Transference number of <math>K^+</math> from</u>		
	<u>Onsager Eq.</u>	<u>Knobel Eq.</u>	<u>Merenkov Eq.</u>
0	0.271	-	0.213
0.03	0.261	0.2633	0.205
0.1	0.251	0.2633	0.198
0.3	0.232	0.2633	0.187
1.0	0.176	0.2633	0.166
3.0	-	0.2633	0.132
5.0	-	-	0.108
7.0	-	-	0.088
9.0	-	-	0.072
10.0	-	-	0.064

5.4 The Primary Hydration Number In Concentrated KOH Solutions

The process of solvation plays an important part in most solution phenomena. The hydration number of an ion is the number of water molecules attached to the ion, and the absolute value of the hydration number has an important bearing on the amount of "free" water present in electrolytic solutions. For example, in 30% KOH solution, if the hydration number of both the potassium and hydroxyl ions is equal to one, then the concentration of "free" water is 36.4 moles/l, while if the hydration number for the ions is equal to four, there will not be

any "free" water available. The concentration of "free" water for different values of the hydration number at various potassium hydroxide concentrations is tabulated in Table 5.2 (assuming that the hydration number of the potassium ion is equal to that of the hydroxyl ion).

Table 5.2

Concentration of "Free" Water  
As A Function Of Hydration Number

Concentration of KOH Solution		Concentration of free water*, $c_{fw}$ , moles/l					
Wt. %	moles/l	s=0	1	2	3	4	5
10	2.3	64.5	59.9	55.3	50.7	46.1	41.2
20	4.6	57.3	48.1	38.9	29.7	20.5	11.3
30	6.9	50.2	36.4	22.6	8.8	-	-
40	9.2	43.0	24.6	6.2	-	-	-
50	11.5	35.8	12.8	-	-	-	-

\* See Appendix 3 for sample calculations.

The concentration of "free" water as a function of KOH concentration is shown in Figure 17 for several arbitrary values of the hydration number.

Many workers have investigated the concept of ionic hydration, and several experimental methods have been used for determining the hydration number of ions. Some of these are discussed below; however, it should be noted that the different experimental methods give contradictory results because of a lack of a really precise definition of the hydration number. As pointed out earlier, solvation is arbitrarily

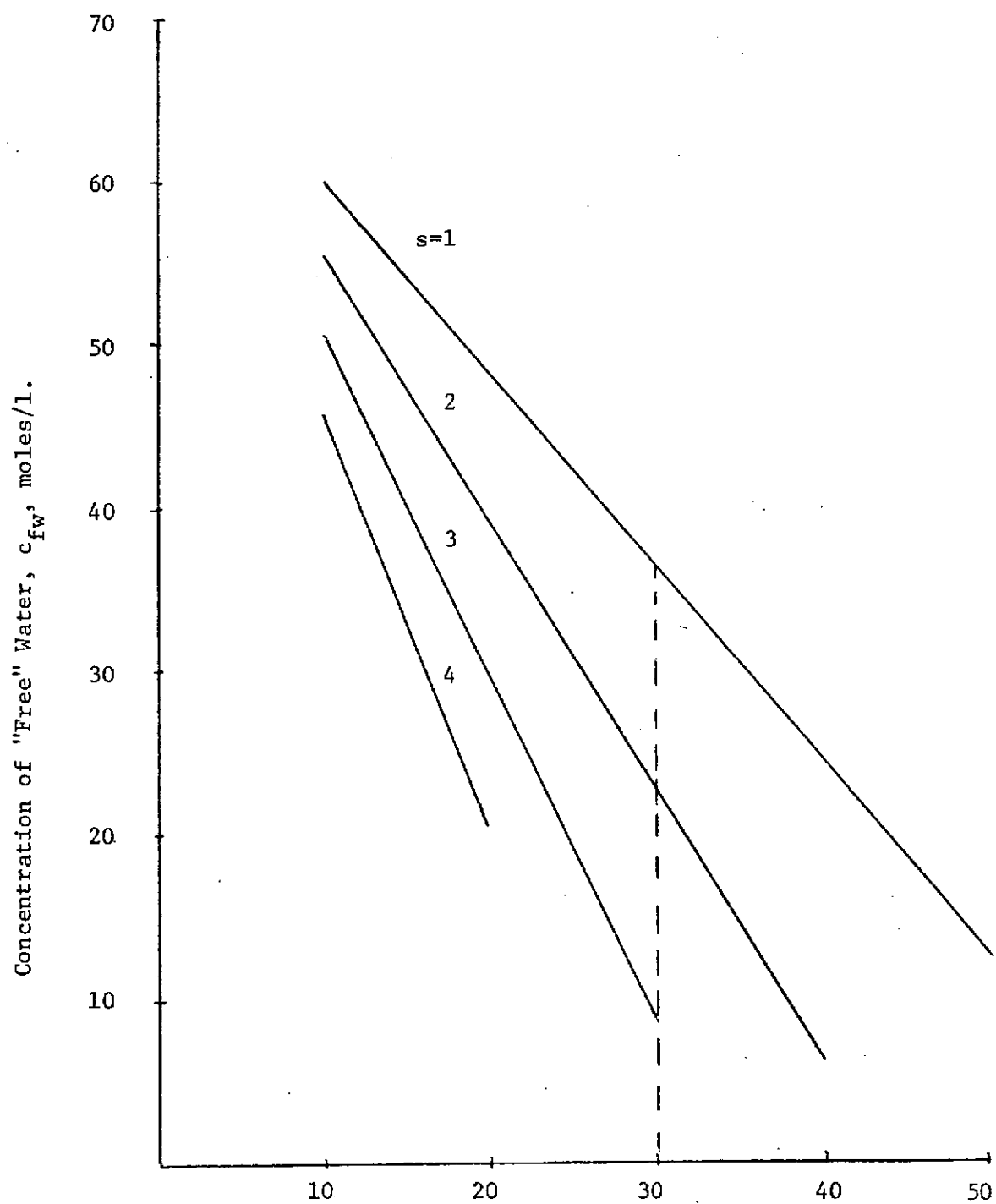


Figure 17: Concentration of "Free" Water in KOH Solution For Different Degrees of Solvation.

divided into two different categories--primary and secondary.

Of the several experimental methods for determining primary hydration numbers which have been used, the more widely used appear to be: ionic entropy, ionic mobility, density, compressibility, and the nuclear magnetic resonance method. Some of the experimental results which have been reported for the hydration number of the potassium ion are summarized in Table 5.3.

Table 5.3

Primary Hydration Numbers of  $K^+$   
By Various Experimental Methods

<u>Method</u>	<u>Hydration Number</u>
<u>Entropy</u> , Ulich (19)	3
<u>Density</u> , Darmois (20)	1
<u>Compressibility</u> , Passynski (21), Bockris (22)	6-7 3.5
<u>nmr</u> , Hindman (23)	2.1
Creekmore et al. (24)	4.6
<u>X-ray diffraction</u> , Brady (25)	4.0

In general there is a great variance in the experimental values of the hydration number because different methods measure different types of solvation (primary or secondary, or a combination of both). Of all the techniques available, nuclear magnetic resonance (nmr) and compressibility appear to be the most promising methods for determining the hydration number of ions.

The use of the nmr techniques for determining the hydration number of ions is still an active field of research, and several approaches can be used to determine the hydration number from nmr measurements. Swinehart and Taube (26) determined the solvation number of certain diamagnetic cations in methanol from the ratio of areas under the nmr absorption curves of the free and solvated molecules. It has been shown by Jackson, Lemons, and Taube (27) that adding a paramagnetic ion to an aqueous solution containing diamagnetic ion produces two separate  $O^{17}$  nuclear magnetic resonances, one for the labile water and the other due to water bound in the primary hydration sheath of the diamagnetic ion. The hydration number of the cation is then determined either by comparing the areas under the two resonances or by measuring the  $O^{17}$  nmr shifts in solutions containing a paramagnetic ion and a diamagnetic ion and in a solution containing only the paramagnetic ion. The hydration number of ions can also be determined by nmr techniques from proton relaxation time measurements.

Although the nuclear magnetic resonance method has become an increasingly important technique for the study of hydration of ions, the feasibility of the technique for measuring the hydration numbers of potassium and hydroxyl ions in concentrated solutions requires further investigation.

The compressibility method, developed by Passynski (21) also appears to be a satisfactory method for determining the hydration number. By assuming the compressibility of water in the primary hydration sheath to be zero, the sum of the hydration number of ions in solution can be determined from compressibility measurements on the

solvent and solution. Isemuro and Goto (28) used the method of compressibility to estimate the hydration number of alkaline halides. As one might expect, they found that the hydration numbers of 1-1 electrolytes decrease with an increase in the temperature, but the concentration dependence of the hydration number was not investigated. Recently, Bockris (22) used the compressibility method to determine the sum of the hydration numbers of ions in solutions of halides. By combining compressibility measurements with measurements of the ionic vibration potential, individual hydration numbers for certain cations and anions were estimated. According to his results, the hydration number of potassium ion is 3.5 and that for hydroxyl ion can be estimated to be equal to 4.3. If these hydration numbers remain constant in concentrated solutions, as pointed out earlier, there would not be any "free" water available in 30% KOH solution. It is obvious, therefore, that the hydration number must vary with the concentration of the solution, but there is little experimental information concerning the concentration dependence of the hydration numbers of the potassium and hydroxyl ions at high concentrations.

From some of the limited information available in Bockris's paper, the hydration number of the potassium and hydroxyl ions may be estimated by extrapolating the available data. This procedure results, for 30% KOH solution, in an estimated hydration number of potassium ion of 1.5 and 2.0 for the hydroxyl ion. These values are, however, very tentative owing to the extrapolation required. Since they are the best estimates available, however, they are used in the next section to estimate concentration gradients in the electrolyte matrix for different current densities.

### 5.5 Concentration Gradients in the Electrolyte Matrix

Having estimated the hydration numbers and the transference numbers of the ions, the flux equations for the potassium ion, the hydroxyl ion, and water can be solved. The concentration gradients of the "free" water and that of the electrolyte in the electrolyte matrix can be estimated as follows:

For the "free" water concentration gradient, we have from Equation 5.2-22

$$N_{H_2O} = -D \frac{dc_{fw}}{dx} + s N_- = \frac{i}{F}$$

Hence the "free" water concentration gradient can be expressed in terms of the hydration number of ions, the diffusivity, and the current density, that is

$$\frac{dc_{fw}}{dx} = - \frac{(1 + s_-)i}{DF} \quad (5.5-1)$$

Values of the diffusion coefficient of the electrolyte at various concentrations, taken from Bhatia's results (29), is shown in Table 5.4.

Table 5.4

#### Diffusivity of KOH Solution at 25°C

<u>Concentration of KOH</u>		<u>D x 10<sup>5</sup> (cm<sup>2</sup>/sec)</u>
<u>Wt. %</u>	<u>moles/l</u>	
10	2.3	3.25
20	4.6	3.60
30	6.9	3.75
40	9.2	3.70
50	11.5	3.65

For 30% KOH solution, the diffusivity of the electrolyte is  $3.75 \times 10^{-5} \text{ cm}^2/\text{sec}$ . With the available data on diffusivity and the estimated values of the hydration number, the concentration gradients of "free" water at different KOH concentrations can be calculated as a function of current density. The results of "free" water concentration gradients are summarized in Table 5.5.

Table 5.5

"Free" Water Concentration Gradients

Hydration No. of Hydroxyl Ion	$-\frac{dc}{dx} \text{ fw}$				
	KOH Concentration				
<u>s<sub>m</sub></u>	<u>c=2.3</u>	<u>4.6</u>	<u>6.9</u>	<u>9.2</u>	<u>11.5</u>
1	0.64i	0.58i	0.55i	0.56i	0.57i
2	0.96i	0.86i	0.83i	0.84i	-
3	1.27i	1.15i	1.10i	-	-
4	1.59i	1.44i	-	-	-
5	1.91i	1.73i	-	-	-

For the concentration gradient of the KOH solution, we have from Equation 5.2-21

$$N_- = -v_- D \left( 1 - \frac{d \ln c_o}{d \ln c} \right) \frac{dc}{dx} + \frac{it_-}{z_- F}$$

From Faraday's Law,

$$N_- = \frac{i}{z_- F}$$



Hence the concentration gradient of KOH solution in the electrolyte matrix is

$$\frac{dc}{dx} = \frac{(1 - t_-) i}{v_- D \left( 1 - \frac{dlnc_o}{dlnc} \right) F} \quad (5.5-2)$$

The term  $\left( 1 - \frac{dlnc_o}{dlnc} \right)$  can be shown to be equal to

$$\left( 1 - \frac{dlnc_o}{dlnc} \right) = \frac{1}{c_o \hat{V}_o} \quad (5.5-3)$$

where  $V_o$  is the partial molar volume of the solvent and is given by

$$\hat{V}_o = \frac{M_o}{\rho - c \frac{d\rho}{dc}} \quad (5.5-4)$$

The density of KOH is 1.1884 gm/cm<sup>3</sup> for 20% KOH solution and 1.2905 gm/cm<sup>3</sup> for 30% KOH solution. If we assume that the density is a linear function of the concentration, we get

$$\begin{aligned} V_o &= \frac{18 \text{ gm/mole}}{1.2905 \text{ gm/cc} - 6.9 \text{ moles/l} \left( \frac{1.2905 - 1.1884}{2.3} \right) \frac{\text{gm/cc}}{\text{mole/l}}} \\ &= 18.23 \text{ cc/mole} \end{aligned}$$

Hence

$$\left( 1 - \frac{dlnc_o}{dlnc} \right) = \frac{1}{50.2 \text{ mole/l} \times \frac{18.23 \text{ gm/cc}}{1000 \text{ cc/l}}} = 1.093$$

Thus, the concentration gradient of the KOH solution in the electrolyte matrix is given by

$$\frac{dc}{dx} = \frac{0.0891}{3.75 \times 10^{-5} \text{ cm}^2/\text{sec} \times 1.093 \times 96500 \text{ amp-sec/mole}}$$

$$= 0.0231 \text{ mole/l/cm.}$$

The concentration gradients of KOH solution at different concentrations can be estimated by the same procedure and the results are summarized in Table 5.6

Table 5.6

KOH Concentration Gradients in the Electrolyte Matrix

<u>Wt.% KOH</u>	<u><math>t_+</math></u>	<u><math>D \times 10^5</math> (cm<sup>2</sup>/sec)</u>	<u><math>1 - \frac{d \ln c_o}{d \ln c}</math></u>	<u><math>\frac{dc}{dx}</math></u>
10	0.142	3.25	0.868	0.0521
20	0.112	3.60	0.965	0.0331
30	0.089	3.75	1.093	0.0231
40	0.070	3.70	1.387	0.0141

From Table 5.6 we can see that, for the estimated values of the transference and hydration numbers, a current density of one ampere per cm<sup>2</sup>, and a mean KOH concentration of 30 Wt.% (6.9 N), the KOH concentration gradient in the electrolyte matrix is 0.023 g mole/l/cm. Since the electrolyte matrix is normally less than one millimeter in thickness, it is clear that the KOH concentration difference between the anode and the cathode even at the high current density of one ampere per cm<sup>2</sup> appears to be almost negligible. Moreover, it is clear

that diffusion and electromigration are entirely adequate to support very high current densities.

#### 5.6 Discussion of Simplifying Assumptions

In calculating the concentration gradients, we have assumed that convection is absent. From the calculations obtained, the concentration gradient of the electrolyte across the matrix is very small. The presence of convection would only reduce the concentration gradient further, therefore, the assumption of no convection has not led to significant errors in estimating the free water concentration gradient. In general, a temperature gradient in the electrolyte matrix could lead to a variation in composition which would promote convection. The temperature gradient can also contribute to changes in transport properties and lead to thermal diffusion. Since the transport rates are large and convection has been shown to be of negligible importance, and since thermal diffusion effects are usually of only secondary importance, the assumption of constant temperature seems reasonable.

## 6. Effectiveness Factors In Fuel Cell Components

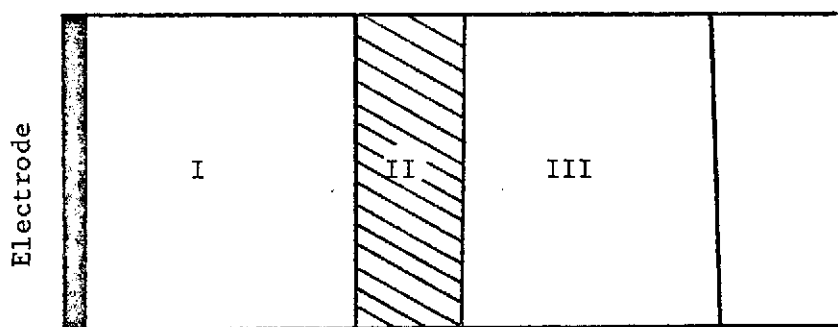
Porous diffusion electrodes are of extremely complex structure, and the sizes of the pores in these electrodes range from 2  $\mu\text{m}$  (2 microns) down to as low as about 2 nm (20 Å). Electrolyte matrices are less complex, but readily accessible to exact analysis. In such cases, the rate of solute diffusion within these pores may become appreciably less than expected when the solute molecular size becomes significant with respect to the pore size. The ratio of the effective diffusivity to the bulk diffusivity of any solute in a porous medium is termed the effectiveness factor,  $\zeta$ . This factor is a function of the porosity and tortuosity of the porous medium, of surface effects, and of possible hindrances to diffusion owing to the size of the diffusing molecules approaching that of the pores. The porosity and tortuosity are macroscopic effects; they correct for the reduction in the area available for diffusion, and the increase in length of the diffusion path, respectively. The other effects are highly complex functions of the molecular properties of the solute and porous medium, and these are not yet well understood. Beck and Schultz (30) as well as Satterfield et al. (31), found that the diffusivity of solutes was reduced when the solute diameter approached the pore diameter in their studies of diffusion through well-defined, homogeneous porous media. On the other hand, Anderson and Quinn (32), and also Wade (34), found no alteration of the transport properties in their studies of the influence of structure of the porous medium on transport processes in pores with sizes comparable to the liquid molecules.

It is evident from these contradictory results, and the lack of understanding of the influence of other parameters on the effectiveness factor in porous electrodes, that experimental measurements of effectiveness factor are necessary for a fuller understanding of transport processes in electrodes, and it is possible that structural influences may be important in the transport processes occurring in electrolyte matrices. The sections following describe a proposed method of evaluating effectiveness factors experimentally and a solution to the mathematical model is given.

#### 6.1 Development of the Model

The proposed experiment involves measuring both the bulk and hindered diffusivities using a modified stagnant microelectrode. With this method only a single measurement is needed for measuring the ratio of bulk and hindered diffusivities.

A schematic diagram of the diffusion cell is shown below.



I is a region where bulk diffusion prevails, II is the sample whose effectiveness factor is to be measured, and III is another region of

bulk diffusion. For such a system, the flux at the electrode can be obtained by solving the following set of differential equations, with the accompanying initial and boundary conditions, for  $t \geq 0$

$$\frac{\partial^2 c_1'}{\partial x^2} - \frac{1}{D_1} \frac{\partial c_1'}{\partial t} = 0 \quad -(\ell_1 + \ell_2) < x < -\ell_2 \quad (6.1-1)$$

$$\frac{\partial^2 c_2'}{\partial x^2} - \frac{1}{D_2} \frac{\partial c_2'}{\partial t} = 0 \quad -\ell_2 < x < 0 \quad (6.1-2)$$

$$\frac{\partial^2 c_3'}{\partial x^2} - \frac{1}{D_3} \frac{\partial c_3'}{\partial t} = 0 \quad 0 < x < \ell_3 \quad (6.1-3)$$

with the following initial and boundary conditions:

Initial condition:  $t \leq 0$ ,  $c_1' = c_2' = c_3' = c_{10}$  for all  $x$ .

Boundary conditions:  $t > 0$

$$c_1' = 0 \quad \text{at } x = -(\ell_1 + \ell_2)$$

$$c_1' = c_2', \quad D_1 \frac{\partial c_1'}{\partial x} = D_2 \frac{\partial c_2'}{\partial x}, \quad \text{at } x = -\ell_2$$

$$c_2' = c_3', \quad D_2 \frac{\partial c_2'}{\partial x} = D_3 \frac{\partial c_3'}{\partial x}, \quad \text{at } x = 0$$

$$c_3' = c_{10} \quad \text{at } x = \ell_3$$

where  $c_1'$ ,  $c_2'$ ,  $c_3'$  are the concentrations in regions I, II, and III, respectively. (They are actual concentrations).  $D_1$ ,  $D_2$ , and  $D_3$  are corrected diffusion coefficients in regions I, II, and III, respectively, i.e., correction is made for the fact that the flux is based on total geometrical area.

The set of equations above can be solved by Laplace Transformation (complete solution is given in Appendix 4), after solving for  $c_1'$ , and given that

$$I_{\text{lim}} = n \text{ FAD}_1 \frac{\partial c_1}{\partial x} \Big|_{x = -(\ell_1 + \ell_2)} \quad (6.1-4)$$

We obtain the following expression for  $I_{\text{lim}}$ :

$$I_{\text{lim}} = \frac{1}{\frac{\ell_1}{D_1} + \frac{\ell_2}{D_2} + \frac{\ell_3}{D_3}} + \sum_{m=0}^{\infty} e^{i \frac{2}{m} t} \frac{\theta_m}{P_m} \quad (6.1-5)$$

where  $\theta_m = K_1 \sin \lambda_m \ell_1 (\cos K_1 \lambda_m \ell_2 \tan K_2 \lambda_m \ell_3 + \sin K_1 \lambda_m \ell_2)$

$$- \cos \lambda_m \ell_1 (K_1^2 \sin K_1 \lambda_m \ell_2 \tan K_2 \lambda_m \ell_3 - K_1 K_2 \cos K_1 \lambda_m \ell_2)$$

$$P_m = K_1 (\ell_1 + \ell_2) \tan K_2 \lambda_m \ell_3 (\sin \lambda_m \ell_1 \cos K_1 \lambda_m \ell_2$$

$$+ K_1 \cos \lambda_m \ell_1 \sin K_1 \lambda_m \ell_2) + K_2 (\ell_1 + \ell_2) \sin \lambda_m \ell_1 \sin K_1 \lambda_m \ell_2$$

$$+ \left( \frac{K_2 \ell_2}{K_1} + K_1 K_2 \ell_1 \right) \cos \lambda_m \ell_1 \cos K_1 \lambda_m \ell_2$$

$$+ \frac{K_1 \ell_3}{K_2} \left( \frac{K_1 \sin \lambda_m \ell_1 \sin K_1 \lambda_m \ell_2 - \cos \lambda_m \ell_1 \cos K_1 \lambda_m \ell_2}{\cos^2 K_2 \lambda_m \ell_3} \right)$$

$$K_1 = \sqrt{\frac{D_2}{D_1}}$$

$$K_2 = \sqrt{\frac{D_3}{D_1}}$$

$\lambda_m$  is given by the equation

$$K_2 \tan K_1 \lambda_m \ell_2 + K_1 \tan \lambda_m K_2 \ell_3 + K_1 K_2 \tan \lambda_m \ell_1$$

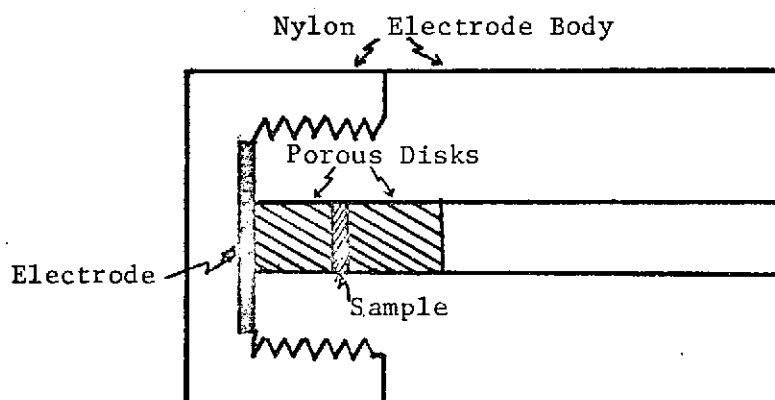
$$= K_1^2 \tan \lambda_m \ell_1 \tan K_1 \lambda_m \ell_2 \tan K_2 \lambda_m \ell_3 = 0$$

## 6.2 Proposed Equipment and Procedure

As noted earlier, the proposed method of measuring effectiveness factors is based on measuring the limiting current with a system approximating a stagnant microelectrode. However, the sample whose effectiveness factor is being evaluated will be sandwiched between two porous disks in which bulk diffusion prevails, i.e., the pores are so large in these regions that there is no hindrance to diffusion in the pore.

In practice we propose, as is often done, to measure the limiting current for an electroactive species whose bulk diffusivity is already known accurately, and for this purpose we have chosen potassium ferrocyanide. We shall make the measurement using 0.05 M  $K_4Fe(CN)_6$  in 0.1 N KCl.

A somewhat enlarged cross-sectional diagram of the cell is shown below.





Porous discs I and III and the porous sample whose effectiveness factor is being measured are fitted into the inside of the cell, and by means of suction the potassium ferrocyanide solution is drawn into the cell. A platinum electrode is then pressed on the surface of disc I by means of a screw-on cap. The experiment can then be started by applying a voltage across the diffusion electrode and a counter electrode while both are immersed in the potassium ferrocyanide solution. A plot of current vs time is generated in the polarograph, and the effectiveness factor of the sample is then calculated from the experimental curve by fitting Equation (6.1-5), using a trial and error procedure on the computer to select appropriate values for  $D_2$ , and noting that (recalling that  $D_1 = D_3$  is already known)

$$\zeta = \frac{D_2}{D_1}$$

## APPENDICES

## APPENDIX 1

### Derivation of Flux Equations (Equations 5.2-11 and 12)

From Faraday's Law, we have

$$\begin{aligned} i &= F \sum_i z_i N_i \\ &= F \sum_i z_i c_i v_i \end{aligned} \quad (\text{A.1-1})$$

Since the solution, as a whole, is electrically neutral, we have

$$\sum_i z_i c_i = 0 \quad (\text{A.1-2})$$

Thus Equation A.1-1 can be written as

$$\begin{aligned} i &= F \sum_i z_i c_i v_i - F \sum_i (z_i c_i) v_o \\ &= F \sum_i z_i c_i (v_i - v_o) \end{aligned} \quad (\text{A.1-3})$$

Therefore, for a 1-1 electrolyte such as KOH, we have

$$i = F z_+ c_+ (v_+ - v_o) + F z_- c_- (v_- - v_o) \quad (\text{A.1-4})$$

From Equations 5.2-6 and 7, we have

$$c_+ \nabla \mu_+ = RT \left( \frac{c_+ c_o}{c_T \phi_{o+}} (v_o - v_+) + \frac{c_- c_+}{c_T \phi_{+-}} (v_- - v_o) \right) \quad (5.2-6)$$

$$c_- \nabla \mu_- = RT \left( \frac{c_- c_o}{c_T \phi_{o-}} (v_o - v_-) + \frac{c_- c_+}{c_T \phi_{+-}} (v_+ - v_-) \right) \quad (5.2-7)$$

Adding the last two equations, we get

$$c_+ \nabla \mu_+ + c_- \nabla \mu_- = \frac{RTc_+c_o}{c_T \mathcal{D}_{O+}} (v_o - v_+) + \frac{RTc_-c_o}{c_T \mathcal{D}_{O-}} (v_o - v_-) \quad (\text{A.1-5})$$

The electrochemical potential of the electrolyte,  $\mu_e$ , is given by

$$\mu_e = v_+ \mu_+ + v_- \mu_- \quad (\text{A.1-6})$$

The stoichiometric concentration of the electrolyte can be written as

$$c = \frac{c_+}{v_+} = \frac{c_-}{v_-} \quad (\text{A.1-7})$$

Hence

$$\begin{aligned} c_+ \mu_+ + c_- \mu_- &= c(v_+ \mu_+ + v_- \mu_-) \\ &= c \nabla \mu_e \end{aligned}$$

Therefore, we get

$$c \nabla \mu_e = \frac{RTc_+c_o}{c_T \mathcal{D}_{O+}} (v_o - v_+) + \frac{RTc_-c_o}{c_T \mathcal{D}_{O-}} (v_o - v_-) \quad (\text{A.1-8})$$

Eliminating  $v_+$  from Equations A.1-4 and 8, we get

$$\begin{aligned} &\frac{RTc_+c_o}{c_T \mathcal{D}_{O+}} + Fz_+c_+c \nabla \mu_e \\ &= \frac{RTc_+c_o}{c_T \mathcal{D}_{O+}} Fz_-c_- (v_- - v_o) + \frac{RTc_-c_o}{c_T \mathcal{D}_{O-}} Fz_+c_+ (v_o - v_-) \\ &= \frac{RTc_o(c_+c_-F)}{c_T} \left( \frac{z_+}{\mathcal{D}_{O+}} - \frac{z_-}{\mathcal{D}_{O-}} \right) (v_o - v_-) \end{aligned}$$

$$= \frac{RTc_o c_+ c_- F}{c_T} \left( \frac{z_+ \delta_{o+} - z_- \delta_{o-}}{\delta_{o+} \delta_{o-}} \right) (v_o - v_-) \quad (\text{A.1-9})$$

Therefore

$$c_- (v_o - v_-) = \frac{iz_- \delta_{o-}}{z_- F (z_+ \delta_{o+} - z_- \delta_{o-})} + \frac{c_T c \nabla \mu_e z_+ \delta_{o+} \delta_{o-}}{RTc_o (z_+ \delta_{o+} - z_- \delta_{o-})} \quad (\text{A.1-10})$$

Substituting Equations 5.2-13 and 14 into Equations A.1-10 we get

$$c_- (v_o - v_-) = - \frac{it_-}{z_- F} + \frac{c_T c \nabla \mu_e}{RTc_o} \frac{z_+}{(z_+ - z_-)} \quad (\text{A.1-11})$$

Since the solution is electrically neutral

$$z_+ c_+ + z_- c_- = 0$$

$$z_+ = - \frac{z_- c_-}{c_+}$$

Hence

$$\begin{aligned} \frac{z_+}{z_+ - z_-} &= \frac{- \frac{z_- c_-}{c_+}}{- \frac{z_- c_-}{c_+} - z_-} \\ &= \frac{c_-}{c_+ + c_-} \\ &= \frac{v_- c}{v_+ c + v_- c} \\ &= \frac{v_-}{v_+ + v_-} \\ &= \frac{v_-}{v} \end{aligned} \quad (\text{A.1-12})$$

Substituting Equation A.1-12 into Equation A.1-11, we get

$$c_{-}(v_o - v_{-}) = - \frac{it_{-}}{z_{-}F} + \frac{c_T c \nabla \mu_e v_{-}}{\nu RT c_o} \quad (A.1-13)$$

Hence

$$c_{-} v_{-} = - \frac{v_{-} \delta c_T}{\nu RT c_o} c \nabla \mu_e + \frac{it_{-}}{z_{-}F} + c_{-} v_o \quad (5.2-12)$$

Similarly, it can be shown that

$$c_{+} v_{+} = - \frac{v_{+} \delta c_T}{\nu RT c_o} c \nabla \mu_e + \frac{it_{+}}{z_{+}F} + c_{+} v_o \quad (5.2-11)$$

## APPENDIX 2

### Derivation of Equation 5.2-16

The electrochemical potential of the electrolyte is given by

$$\mu_e = \nu RT \ln(cf_{\pm} a_{\pm}^{\theta}) \quad (\text{A.2-1})$$

where  $f_{\pm}$  is the mean molar activity coefficient of the electrolyte and  $a_{\pm}^{\theta}$  is a proportionality constant. The gradient of the electrochemical potential of the electrolyte is then given by

$$\begin{aligned} \nabla \mu_e &= \nu RT \frac{\partial}{\partial x} \ln(cf_{\pm} a_{\pm}^{\theta}) \\ &= \frac{\nu RT}{cf_{\pm} a_{\pm}^{\theta}} \left( f_{\pm} a_{\pm}^{\theta} \frac{\partial c}{\partial x} + c a_{\pm}^{\theta} \frac{\partial f_{\pm}}{\partial x} \right) \\ &= \frac{\nu RT}{cf_{\pm}} \left( f_{\pm} + c \frac{\partial f_{\pm}}{\partial c} \right) \nabla c \end{aligned} \quad (\text{A.2-2})$$

Therefore

$$\begin{aligned} \frac{c \nabla \mu_e}{\nu RT} &= \left( 1 + \frac{c \partial f_{\pm}}{f_{\pm} \partial c} \right) \nabla c \\ &= \left( 1 + \frac{\partial \ln f_{\pm}}{\partial \ln c} \right) \nabla c \end{aligned}$$

Thus

$$\frac{\partial c_T}{\nu RT c_o} c \nabla \mu_e = \left( \frac{\partial c_T}{c_o} \right) \left( 1 + \frac{d \ln f_{\pm}}{d \ln c} \right) \nabla c \quad (\text{A.2-3})$$

The measured diffusion coefficient of the electrolyte,  $D$ , is related to  $\mathcal{D}$  by

$$D = \mathcal{D}(1 + vM_o m) \left(1 + \frac{d \ln \gamma_{\pm}}{d \ln m}\right) \quad (\text{A.2-4})$$

$\therefore$

$$v = v_+ + v_-$$

$$m = \frac{c}{\rho - \sum_{j=0} c_j M_j} = \frac{c}{c_o M_o} \quad (\text{A.2-5})$$

Therefore

$$\begin{aligned} D &= \mathcal{D} \left\{ 1 + (v_+ + v_-) M_o \frac{c}{c_o M_o} \right\} \left( 1 + \frac{d \ln \gamma_{\pm}}{d \ln m} \right) \\ &= \mathcal{D} \left\{ \frac{c_o + c_+ + c_-}{c_o} \right\} \left( 1 + \frac{d \ln \gamma_{\pm}}{d \ln m} \right) \\ &= \mathcal{D} \frac{c_T}{c_o} \left( 1 + \frac{d \ln \gamma_{\pm}}{d \ln m} \right) \end{aligned} \quad (\text{A.2-6})$$

Hence we get

$$\frac{\mathcal{D} c_T}{v R T c_o} c \nabla \mu_e = \frac{D \left( 1 + \frac{d \ln f_{\pm}}{d \ln c} \right)}{\left( 1 + \frac{d \ln \gamma_{\pm}}{d \ln m} \right)} \nabla c \quad (\text{A.2-7})$$

The measured diffusion coefficient of the electrolyte,  $D$ , is also related to  $\mathcal{D}$  by the following relation

$$D = \frac{\mathcal{D} \frac{1 + vM_o m}{1 + Mm} \left( 1 + \frac{d \ln f_{\pm}}{d \ln c} \right)}{\left( 1 - \frac{d \ln \rho}{d \ln c} \right)} \quad (\text{A.2-8})$$

From Equations A.2-4 and 8, we get



$$\begin{aligned}
\frac{1 + \frac{d \ln f_{\pm}}{d \ln c}}{1 + \frac{d \ln \gamma_{\pm}}{d \ln m}} &= (1 + M_m) \left( 1 - \frac{d \ln \rho}{d \ln c} \right) \\
&= \left( 1 + \frac{M_c}{c_o M_o} \right) \left( 1 - \frac{d \ln \rho}{d \ln c} \right) \\
&= 1 + \frac{M_c}{c_o M_o} - \left( 1 + \frac{M_c}{\rho_o} \right) \frac{d \ln \rho}{d \ln c} \\
&= 1 + \frac{M_c}{c_o M_o} - \frac{\rho_o d \ln \rho}{\rho_o d \ln c} \\
&= 1 - \left( \frac{\rho_o d \ln \rho}{\rho_o d \ln c} - \frac{M_c}{\rho_o} \right) \tag{A.2-9}
\end{aligned}$$

$$\therefore \rho = c_o M_o + M_c$$

$$\begin{aligned}
\frac{d \ln \rho}{d c} &= \frac{1}{c_o M_o + M_c} \frac{\partial}{\partial c} (c_o M_o + M_c) \\
&= \frac{1}{\rho} M_o \frac{\partial c_o}{\partial c} + \frac{M}{\rho}
\end{aligned}$$

Multiplying each side of the above equation by  $c$ , we get

$$\begin{aligned}
\frac{d \ln \rho}{d \ln c} &= \frac{c}{\rho} M_o \frac{\partial c_o}{\partial c} + \frac{M_c}{\rho} \\
&= \frac{c \rho_o \partial c_o}{c_o \rho \partial c} + \frac{M_c}{\rho} \\
&= \frac{\rho_o \ln c_o}{\rho \ln c} + \frac{M_c}{\rho} \tag{A.2-10}
\end{aligned}$$

Substituting Equation A.2-10 into Equation A.2-9, we get

$$\begin{aligned}
\frac{1 + \frac{d \ln f_{\pm}}{d \ln c}}{1 + \frac{d \ln \gamma_{\pm}}{d \ln m}} &= 1 - \left( \frac{\rho}{\rho_o} \left( \frac{\rho_o}{\rho} \frac{d \ln c_o}{d \ln c} + \frac{M_c}{\rho} \right) - \frac{M_c}{\rho_o} \right) \\
&= 1 - \left( \frac{d \ln c_o}{d \ln c} + \frac{M_c}{\rho_o} - \frac{M_c}{\rho_o} \right) \\
&= 1 - \frac{d \ln c_o}{d \ln c} \quad (A.2-11)
\end{aligned}$$

Substituting Equation A.2-11 into Equation A.2-7, we thus get

$$\frac{\theta c_T}{v R T c_o} c \nabla \mu_e = D \left( 1 - \frac{d \ln c_o}{d \ln c} \right) \nabla c \quad (5.2-16)$$

### APPENDIX 3

#### Sample Calculation of "Free" Water Concentration

The amount of "free" water for a given electrolytic solution is equal to the portion of water that is not tightly bound in the primary hydration sheaths of the ion. Hence the concentration of "free" water is the concentration difference before and after hydration of ions.

For 30% KOH solution, the concentration of KOH and water before hydration are as follows:

$$\begin{aligned} \text{Concentration of KOH, } c &= \frac{30 \text{ gm}}{100 \text{ gm soln}} \times 1.29 \frac{\text{gm soln}}{\text{cc}} \times 1000 \frac{\text{cc}}{\text{l}} \\ &\quad 56.1 \frac{\text{gm}}{\text{mole}} \\ &= 6.9 \text{ gm/l} \end{aligned}$$

The molar concentration of water

$$\begin{aligned} &= \frac{(100 - 30) \text{ gm}}{100 \text{ gm soln}} \times 1.29 \frac{\text{gm soln}}{\text{cc}} \times 1000 \frac{\text{cc}}{\text{l}} \\ &\quad 18 \frac{\text{gm}}{\text{mole}} \\ &= 50.2 \text{ mole/l} \end{aligned}$$

If the hydration number of the potassium ion and that of the hydroxyl ion are assumed to be equal, then the concentration of "free" water is given by

$$\begin{aligned} c_{fw} &= c_{tw} - c_{bw} \\ &= c_{tw} - 2sc \end{aligned}$$

where  $c_{tw}$  is the concentration of total water, that is, the concentration of water before hydration;  $c_{bw}$  is the concentration of bound water.

If the hydration number of the ions is equal to one, then

$$\begin{aligned} c_{fw} &= 50.2 \text{ mole/l} - (2)(1)(6.9) \text{ mole/l} \\ &= 36.4 \text{ mole/l} \end{aligned}$$

Values of the concentration of "free" water are summarized in Table 5.2.

#### APPENDIX 4

##### Solution of the Diffusion Equation For the Effectiveness Factor Cell

The set of equations to be solved is, for  $t > 0$

$$\frac{\partial^2 c_1'}{\partial x^2} - \frac{1}{D_1} \frac{\partial c_1'}{\partial t} = 0 \quad -(\ell_1 + \ell_2) < x < -\ell_2$$

$$\frac{\partial^2 c_2'}{\partial x^2} - \frac{1}{D_2} \frac{\partial c_2'}{\partial t} = 0 \quad -\ell_2 < x < 0$$

$$\frac{\partial^2 c_3'}{\partial x^2} - \frac{1}{D_3} \frac{\partial c_3'}{\partial t} = 0 \quad 0 < x < \ell_3$$

where the concentrations are based on the actual concentration in the pores, and the diffusion coefficients are those corrected for the differences in diffusion surface area.

The boundary and initial conditions for the above system are:

Initial Conditions:  $t \leq 0$

$$c_1' = c_2' = c_3' = c_{10}$$

Boundary Conditions:  $c_1' = 0$  at  $x = -(\ell_1 + \ell_2)$

$$c_1' = c_2'$$

$$D_1 \frac{\partial c_1'}{\partial x} = D_2 \frac{\partial c_2'}{\partial x}$$

at  $x = -\ell_2$

$$\left. \begin{aligned} c_2' &= c_3' \\ D_2 \frac{\partial c_2'}{\partial x} &= D_3 \frac{\partial c_3'}{\partial x} \end{aligned} \right\} \text{ at } x = \ell_3$$

First, we make the transformation

$$c_1 = c_1' - c_{10}$$

$$c_2 = c_2' - c_{10}$$

$$c_3 = c_3' - c_{10}$$

The above equations are transformed into

$$\frac{\partial^2 c_1}{\partial x^2} - \frac{1}{D_1} \frac{\partial c_1}{\partial t} = 0 \quad -(\ell_1 + \ell_2) < x < -\ell_2 \quad (\text{A.4-1})$$

$$\frac{\partial^2 c_2}{\partial x^2} - \frac{1}{D_2} \frac{\partial c_2}{\partial t} = 0 \quad -\ell_2 < x < 0 \quad (\text{A.4-2})$$

$$\frac{\partial^2 c_3}{\partial x^2} - \frac{1}{D_3} \frac{\partial c_3}{\partial t} = 0 \quad 0 < x < \ell_3 \quad (\text{A.4-3})$$

Initial Condition  $t \leq 0$

$$c_1 = c_2 = c_3 = 0$$

Boundary Condition:  $t > 0$

$$c_1 = c_{1s} (= -c_{10}) \quad \text{at } x = -(\ell_1 + \ell_2) \quad (\text{A.4-4})$$

$$c_1 = c_2, \quad D_1 \frac{\partial c_1}{\partial x} = D_2 \frac{\partial c_2}{\partial x} \quad x = -\ell_2$$

$$c_2 = c_3, \quad D_2 \frac{\partial c_2}{\partial x} = D_3 \frac{\partial c_3}{\partial x} \quad x = 0$$

$$c_3 = 0 \quad x = \ell_3$$

To solve Equations A.4-1, 2, and 3, with the given Initial Conditions and Boundary Conditions, they are Laplace Transformed, and solved to give

$$\bar{c}_1 = \frac{c_{1s}}{p} \cosh q_1 (\ell_1 + \ell_2 + x) + A \sinh q_1 (\ell_1 + \ell_2 + x) \quad (\text{A.4-8})$$

$$\bar{c}_2 = B \cosh q_2 (\ell_2 + x) + C \sinh q_2 (\ell_2 + x) \quad (\text{A.4-9})$$

$$\bar{c}_3 = E (\sinh q_3 x - \tanh q_3 \ell_3 \cosh q_3 x) \quad (\text{A.4-10})$$

where

$$q_1 = \sqrt{p/D_1}$$

$$q_2 = \sqrt{p/D_2}$$

$$q_3 = \sqrt{p/D_3}$$

$p$  = the parameter for the Laplace Transformation.

A, B, C and D are constants to be evaluated from the Boundary Conditions (A.4-5 and 6). It should be noted that conditions A.4-4 and 7 have been used to obtain Equations A.4-8 through 10.

Substitution of Equations A.4-8 through 10 into the Boundary Conditions give

$$\frac{c_{1s}}{p} = \cosh q_1 \ell_1 + A \sinh q_1 \ell_1 = B \quad (\text{A.4-11})$$

$$\frac{c_{1s}}{p} = D_1 q_1 \sinh q_1 \ell_1 + A q_1 D_2 \cosh q_1 \ell_1 = c q_2 D_2 \quad (\text{A.4-12})$$

$$B \cosh q_2 \ell_2 + c \sinh q_2 \ell_2 = -E \tanh q_3 \ell_3 \quad (\text{A.4-13})$$

$$B q_2 D_2 \sinh q_2 \ell_2 + c q_2 D_2 \cosh q_2 \ell_2 = E D_3 q_3 \quad (\text{A.4-14})$$

Solving Equations A.4-11 through 14 for A gives

$$A = \frac{c_{1s}}{p} \{ M/N \} \quad (\text{A.4-15})$$

$$\begin{aligned} \text{where } M &= D_1 q_1 \sinh q_1 \ell_1 (D_3 q_3 \sinh q_2 \ell_2 + D_2 q_2 \cosh q_2 \ell_2) \\ &\quad + D_2 q_2 \cosh q_1 \ell_1 (D_3 q_3 \cosh q_2 \ell_2 + D_2 q_2 \sinh q_2 \ell_2 \tanh q_3 \ell_3) \\ N &= D_1 q_1 \cosh q_1 \ell_1 (D_3 q_3 \sinh q_2 \ell_2 + D_2 q_2 \cosh q_2 \ell_2 \tanh q_3 \ell_3) \\ &\quad + D_2 q_2 \sinh q_1 \ell_1 (D_3 q_3 \cosh q_2 \ell_2 + D_2 q_2 \sinh q_2 \ell_2 \tanh q_3 \ell_3) \end{aligned}$$

Only A was solved for because we are interested in  $\bar{c}_1$  which contains A as the sole constant to be evaluated.

Substituting Equation A.4-15 to Equation A.4-8 yields

$$\frac{\bar{c}_1}{c_{1s}} = \frac{1}{p} \left[ K/L \right] \quad (\text{A.4-16})$$

$$\begin{aligned} \text{where } K &= D_1 q_1 (D_3 q_3 \sinh q_2 \ell_2 + D_2 q_2 \cosh q_2 \ell_2 \tanh q_3 \ell_3) \cosh q_1 (2\ell_1 + \ell_2 + x) \\ &\quad - D_2 q_2 (D_3 q_3 \cosh q_2 \ell_2 + D_2 q_2 \sinh q_2 \ell_2 \tanh q_3 \ell_3) \sinh q_1 (2\ell_1 + \ell_2 + x) \end{aligned}$$



$$L = D_1 q_1 (D_3 q_3 \sinh q_2 \ell_2 + D_2 q_2 \cosh q_2 \ell_2 \tanh q_3 \ell_3) \cosh q_1 \ell_1 \\ + D_2 q_2 (D_3 q_3 \cosh q_2 \ell_2 + D_2 q_2 \sinh q_2 \ell_2 \tanh q_3 \ell_3) \sinh q_1 \ell_1$$

$c_1$  can be obtained by means of the Inversion Theorem. We see that Equation A.4-16 gives a simple pole, and zeros of "L" give simple poles of the integrand of Equation A.4-16 in the inversion equation.

$$\therefore \frac{c_1}{c_{1s}} = \text{Res}(0) + \sum_{m=1}^{\infty} \text{Res}(-D_1 \lambda_m^2)$$

We see that  $\text{Res}(0) = 0/0$ ; therefore, we have to apply L'Hopital's rule, which, after simplification, gives

$$\text{Res}(0) = \frac{D_1 D_3 \ell_2 + D_1 D_2 \ell_3 - D_2 D_3 (\ell_2 + x)}{D_1 D_3 \ell_2 + D_1 D_2 \ell_3 + D_2 D_3 \ell_1}$$

$$\text{Res}(-D_1 \lambda_m^2) = \frac{K(-D_1 \lambda_m^2)}{-D_1 \lambda_m^2 (\partial L / \partial p)_{p=-D_1 \lambda_m^2}} \quad (\text{By using L'Hopital's rule})$$

$$\text{Letting } K_1 = \sqrt{D_2/D_1}, \quad K_2 = \sqrt{D_3/D_1}, \quad p = -D_1 \lambda_m^2$$

$$K(-D_1 \lambda_m^2) = i e^{-i \lambda_m^2 t} \left( \sqrt{D_1 D_2} \cos \lambda (2\ell_1 + \ell_2 + x) \cos K_1 \lambda t \tan K_2 \lambda t_3 \right. \\ + \sqrt{D_1 D_2} \cos \lambda (2\ell_1 + \ell_2 + x) \sin K_1 \lambda \ell_2 - \frac{D_2 D_3}{\sqrt{D_1 D_2}} \sin \lambda (\ell_2 + x) \cos K_1 \lambda \ell_2 \\ \left. + D_2 \sin \lambda K_1 \ell_2 \sin \lambda (\ell_2 + x) \tan K_2 \lambda \ell_3 \right)$$

$$\begin{aligned}
\frac{dL}{dp} \Big|_{p=-D_1}^2 = \frac{1}{2i} & \left\{ \begin{aligned} & -K_1 \ell_1 \sin \lambda \ell_1 \cos \lambda K_1 \ell_2 \tan \lambda K_2 \ell_3 \\ & -\ell_2 \cos \lambda \ell_1 \sin \lambda K_1 \ell_2 \tan \lambda K_2 \ell_3 \end{aligned} \right. \\
& + \frac{K_1}{K_2} \frac{\cos \lambda \ell_1 \cos \lambda K_1 \ell_3}{\cos^2 \lambda K_2 \ell_3} - K_2 (\ell_1 + \ell_2) \sin \lambda \ell_1 \sin \lambda K_1 \ell_2 \\
& + \frac{K_2}{K_1} \ell_2 \cos \lambda \ell_1 \cos \lambda K_1 \ell_2 + K_1 K_2 \ell_1 \cos \lambda \ell_1 \cos \lambda K_1 \ell_2 \\
& - K_1^2 \ell_1 \cos \lambda \ell_1 \sin \lambda K_1 \ell_2 \tan \lambda K_2 \ell_3 - K_1 \ell_2 \sin \lambda \ell_1 \cos \lambda K_1 \ell_2 \tan \lambda K_2 \ell_3 \\
& - \frac{K_1^2}{K_2} \frac{\sin \lambda \ell_1 \sin \lambda K_1 \ell_2}{\cos^2 \lambda K_2 \ell_3} \Big\}
\end{aligned}$$

$$\therefore \frac{c_1}{c_{1s}} = \frac{D_1 D_3 \ell_2 + D_1 D_2 \ell_3 - D_2 D_3 (\ell_2 + x)}{D_1 D_3 \ell_2 + D_1 D_2 \ell_3 + D_2 D_3 \ell_1} - \sum_m 2e^{D_1 \lambda_m^2 t} \frac{\theta_m}{P_m}$$

$$\text{where } \theta_m = \{K_1 \cos \lambda_m (2\ell_1 + \ell_2 + x) (\cos K_1 \lambda_m \ell_2 \tan K_2 \lambda_m \ell_3$$

$$+ \sin K_1 \lambda_m \ell_2) + \sin \lambda_m (\ell_2 + x) (K_1^2 \sin K_1 \lambda_m \ell_2 \tan K_2 \lambda_m \ell_3$$

$$- K_1 K_2^2 \cos K \lambda_m \ell_2) \}$$

$$\begin{aligned}
P_m = D_1 \lambda_m & \left\{ K_1 (\ell_1 + \ell_2) \sin \lambda_m \ell_1 \cos \lambda_m K_1 \ell_2 \tan \lambda_m K_2 \ell_3 \right. \\
& + K_1^2 (\ell_1 + \ell_2) \cos \lambda_m \ell_1 \sin \lambda_m K_1 \ell_2 \tan \lambda_m K_2 \ell_3 \\
& + K_2 (\ell_1 + \ell_2) \sin \lambda_m \ell_1 \sin \lambda_m K_1 \ell_2 - \left[ \frac{K_2 \ell_2}{K_1} + K_1 K_2 \ell_1 \right] \\
& \left. \cos \lambda_m \ell_1 \cos \lambda_m K_1 \ell_2 + \frac{K_1 \ell_3}{K_2} \frac{(K_1 \sin \lambda_m \ell_1 \sin \lambda_m - \cos \lambda_m \ell_1 \cos \lambda_m K_1 \ell_2)}{\cos^2 \lambda_m K_2 \ell_3} \right\}
\end{aligned}$$

where  $\lambda_m$  are given by solution of the equation

$$K_2 \tan K_1 \lambda \ell_2 + K_1 \tan K_2 \lambda \ell_3 + K_1 K_2 \tan \lambda \ell_1 \\ + K_1^2 \tan K_1 \lambda \ell_2 \tan K_2 \lambda \ell_3 \tan \lambda \ell_1 = 0$$

since

$$I_{lim} = nFA D_1 \left. \frac{\partial c_1}{\partial x} \right|_{x = -\ell_1 - \ell_2}$$

Finally, we have

$$\frac{I_{lim}}{c_{10} nFA} = \frac{1}{\frac{\ell_1}{D_1} + \frac{\ell_2}{D_2} + \frac{\ell_3}{D_3}} + 2 \sum_m e^{i\lambda_m^2 t} \frac{\theta_m}{P_m}$$

#### LIST OF REFERENCES

1. Feldkamp, K., *Chemie. Ing. Tech.*, 41, 1181 (1969).
2. *International Critical Tables*, 1st Ed., IV, 466 (1928).
3. Faust, Von O., *Zeit. Anorg. Chem.*, 160, 373 (1927).
4. Walker, R. D., Fifteenth Semi-Annual Report, September, 1973, NASA Research Grant NGR 10-005-022.
5. Kordesch, K. V., From Electrocatalysis to Fuel Cells. Washington: Washington University Press, (1972), p. 157.
6. Miller, M. L., and Fornasar, H. J., *J. Electrochem. Soc.*, 115 330 (1968).
7. Lundquist, J. T., and Vogel, W. M., *Ibid.*, 116, 1066 (1969).
8. Bockris, J. O'M, *Quart. Rev. (London)* 3, 173 (1949).
9. Hirschfelder, J. O., Curtiss, C. F., and Bird, R. B., Molecular Theory of Gases and Liquids, New York: John Wiley & Sons, Inc., (1954) p. 718.
10. Bird, R. B., Stewart, W. E., and Lightfoot, E. N., Transport Phenomena. New York: John Wiley & Sons, Inc., (1960) p. 570.
11. MacInnes, D. A., and Dole, M., *J. Am. Chem. Soc.*, 53, 1357 (1931).
12. Jones, G., and Bradshaw, B. C., *Ibid.*, 54, 138 (1932).
13. MacInnes, D. A., and Longworth, L. G., *Chem. Rev.*, 11, 171 (1932).
14. Jones, G., and Dole, M., *J. Am. Chem. Soc.*, 51, 1073 (1929).
15. Longworth, L. G., *Ibid.*, 54, 2741 (1932).
16. Owen, B. B., *Ibid.*, 57, 2441 (1935).
17. Merenkov, P. T., *Uzbeksh Khim. Zn.* 50, (1961).
18. Knobel, N., et al., *J. Am. Chem. Soc.*, 45, 77 (1923).
19. Ulich, H., *Z. Elektrochem.*, 36, 497 (1930).
20. Darmais, E., *J. Phys. Radium*, 8, 117 (1942).

21. Passynski, A., Acta Physiocochem., 8, 385 (1938).
22. Bockris, J. O'M., and Saluja, P. P. S., J. Phys. Chem., 76, 2140 (1972).
23. Hindman, J. C., J. Chem. Phys., 36, 1000 (1962).
24. Creekmore, R. W., and Reilly, C. N., J. Phys. Chem., 73, 1563 (1969).
25. Brady, G. W., and Krause, J. T., J. Chem. Phys., 27, 304 (1962).
26. Swinehart, J. H., and Taube, H., J. Phys. Chem., 31, 1579 (1962).
27. Jackson, J. A., and Lemons, J. F., and Taube, H., J. Chem. Phys., 32, 553 (1960).
28. Isemura, Toshizo, and Goto, Sachio, Bulletin of the Chemical Society of Japan, 37, 1690 (1964).
29. Bhatia, R. N., M. S. E. Thesis, University of Florida (1960).
30. Beck, R. E., and J. S. Schultz, Science, 170, 1302 (1970).
31. Satterfield, C. N., C. K. Colton and W. H. Pitcher, A. I. Ch. E. J., 19, 628 (1973).
32. Anderson, J. L. and J. A. Quinn, Trans. Farad. Soc. I. 68, 744 (1972).
33. Wade, W. H., Soc. Pet. Eng. of A. I. M. E. SPE 4364 (1973).
34. Walker, R. D., Sixth Semi-Annual Report, February, 1969, NASA Research Grant NGR 10-005-022.